

Invited Review Article: Single-photon sources and detectors

Cite as: Rev. Sci. Instrum. **82**, 071101 (2011); <https://doi.org/10.1063/1.3610677>

Submitted: 14 December 2010 • Accepted: 07 June 2011 • Published Online: 27 July 2011

M. D. Eisaman, J. Fan, A. Migdall, et al.



ARTICLES YOU MAY BE INTERESTED IN

[Single-photon detectors combining high efficiency, high detection rates, and ultra-high timing resolution](#)



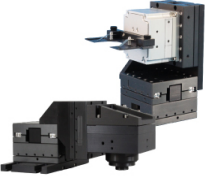
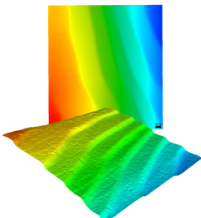
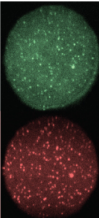
APL Photonics **2**, 111301 (2017); <https://doi.org/10.1063/1.5000001>

[Trapped-ion quantum computing: Progress and challenges](#)

Applied Physics Reviews **6**, 021314 (2019); <https://doi.org/10.1063/1.5088164>

[Toward large-scale fault-tolerant universal photonic quantum computing](#)

APL Photonics **4**, 060902 (2019); <https://doi.org/10.1063/1.5100160>

 <p>MAD CITY LABS INC. www.madcitylabs.com</p>	<p>Nanopositioning Systems</p> 	<p>Modular Motion Control</p> 	<p>AFM and NSOM Instruments</p> 	<p>Single Molecule Microscopes</p> 
--	--	--	---	--

Invited Review Article: Single-photon sources and detectors

M. D. Eisaman,^{a)} J. Fan, A. Migdall, and S. V. Polyakov

*National Institute of Standards and Technology, Gaithersburg, Maryland 20899, USA
and Joint Quantum Institute, University of Maryland, College Park, Maryland 20742, USA*

(Received 14 December 2010; accepted 7 June 2011; published online 27 July 2011)

We review the current status of single-photon-source and single-photon-detector technologies operating at wavelengths from the ultraviolet to the infrared. We discuss applications of these technologies to quantum communication, a field currently driving much of the development of single-photon sources and detectors. © 2011 American Institute of Physics. [doi:10.1063/1.3610677]

I. INTRODUCTION

A. What is a photon?

A photon is defined as an elementary excitation of a single mode of the quantized electromagnetic field.¹ The concept of quantized electromagnetic radiation² was first introduced by Planck in 1900 to explain the black-body radiation spectrum.^{3–5} It was also used by Einstein in 1905 to explain the photoelectric effect^{5–7} and by Compton in 1923 to explain the wavelength shift of scattered x-rays.⁸ The term “photon” was first introduced by G. N. Lewis in 1926.⁹ The formal quantization of the electromagnetic field was first performed by Dirac in 1927.^{10,11}

The mode k of the quantized electromagnetic field is labeled by its frequency ν_k , and a single photon in mode k has energy equal to $h\nu_k$, where h is Planck’s constant. While the monochromatic definition of a photon implies delocalization in time, in practice one often talks about propagating “single-photon states” that are localized to some degree in time and space. Mathematically, one can describe such states as superpositions of monochromatic photon modes.¹ Much discussion can be found in the literature about the definition of a “photon wavefunction.”¹² For the purposes of this review, we adopt the following operational definition of a single-photon state: given a detector that can determine the number of incident photons (in some finite-width frequency range) with 100% accuracy, a single-photon state is an excitation of the electromagnetic field (localized to some degree in both space and time) such that the detector measures exactly one photon for each incident state. Put another way, a single-photon state is one for which the photon-number statistics have a mean value of one photon and a variance of zero. In addition, since the results of quantum measurements may depend on the measurement procedure and apparatus, the physics of the measurement process itself must also be considered.¹³ Single-photon detectors typically work by sensing an electrical signal that results from the absorption of a photon.

B. Why produce and detect single photons?

A major driver of the current research into single-photon sources and single-photon detectors is the explosive growth

of the field of quantum-information science over the last few decades.^{14,15} At its core, quantum-information science involves the encoding, communication, manipulation, and measurement of information using quantum-mechanical objects. Research has shown that using quantum objects for this purpose allows certain computational tasks to be performed more efficiently than thought possible using classical objects,¹⁶ and potentially allows unconditionally secure communication.¹⁷ Photonic qubits, where information is encoded in the quantum state of the photon using degrees of freedom such as polarization, momentum, energy, etc., are an ideal choice for many of these applications, since (a) photons travel at the speed of light and interact weakly with their environment over long distances, which results in lower noise and loss and (b) photons can be manipulated with linear optics.

While quantum communication applications often make use of single photons, many quantum cryptography protocols, in the form of quantum key distribution (QKD) in particular, demand *single* photons traveling over a channel,^{17–19} as more than one photon can compromise the security of the communication by allowing an eavesdropper to gain information.^{20,21} While subsequent schemes, such as those that rely on decoy states^{22–24} and privacy amplification,^{25–28} have been shown to relax this single-photon requirement and to reduce the potential leakage of information to an eavesdropper, quantum cryptography has been a significant driver of single-photon source development. And certainly it is the case that long distance QKD, which requires quantum repeaters,^{29–33} is likely to rely heavily on single photons. Some quantum computation protocols also require single photons, and in addition require that all single photons used in the protocol be indistinguishable from one another.³⁴ Because these quantum protocols require single photons, it is advantageous to employ single-photon detectors that ideally can determine the number of photons in a given pulse. Another single-photon-detection application that has come out of QKD, but has applications in other non-quantum-related fields, is the production of truly random numbers. Light provides a natural solution to this problem, where single photons encountering a beam-splitter exhibit inherent quantum randomness in which output path they take.^{28,35,36} Extracting this path information requires single-photon detection. These requirements, coupled with the strong growth of quantum-information applications (Fig. 1), have provided motivation for the development of improved single-photon sources²⁸ and single-photon detectors.³⁷

^{a)}Present address: Brookhaven National Laboratory, Upton, NY 11973, USA.

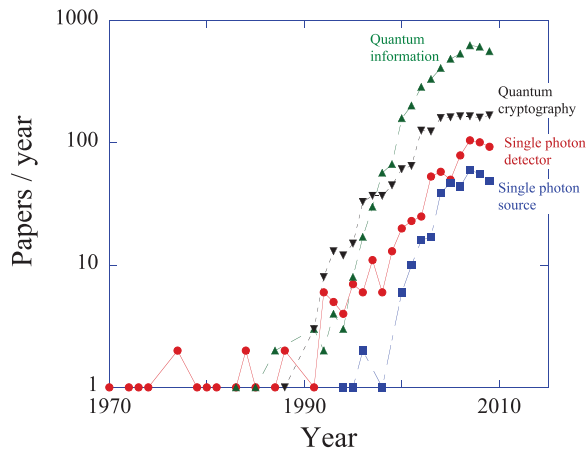


FIG. 1. (Color) Papers published each year. ISI Web of Knowledge search terms are shown.

In addition to quantum-information science, single-photon detectors are used for a wide range of applications, including bioluminescence detection,³⁸ DNA sequencing,^{39–42} Förster resonance energy transfer (FRET) for studying protein folding,^{43–45} light detection and ranging (LIDAR) for remote sensing,^{46,47} and light ranging on shorter scales,⁴⁸ optical time domain reflectometry,^{49–55} picosecond imaging circuit analysis,^{56–61} single-molecule spectroscopy^{62–68} and fluorescence-lifetime measurements,⁶⁹ medical applications such as diffuse optical tomography⁷⁰ and positron emission tomography,⁷¹ and finally applications such as traditional and quantum-enabled metrology.^{72–80}

This review attempts to describe the state-of-the-art of single-photon sources and detectors over the broad range of fields in which these technologies are employed. We have attempted to make the review accessible to those who are new to the field, while at the same time serving as a valuable reference to experts. More specific reviews focused on quantum-metrology applications,⁷⁹ quantum-information applications,⁸¹ fluorescence lifetime determination,⁸² quantum-dot/photonic-crystal sources,⁸³ single-emitter sources,⁸⁴ cavity-based sources,⁸⁵ single-photon sources generally,^{86,87} and solid-state single-photon detectors⁸⁸ may also be of interest to the reader.

C. A brief history of single-photon sources and detectors

Historically, the first detectors able to register single optical photons were photomultiplier tubes (PMTs), which combined the photoelectric cell with an electron multiplier. While early on, Hertz⁸⁹ studied the effect of light on an electrical discharge, and others developed what evolved into the photoelectric cell (see, for example, the work of Elster and Geitel⁹⁰), it was not until the development of the electron multiplier that the signal from a single photon could be observed. As part of an intense race to develop a workable electronic television, a photosensitive element and an electron multiplier were combined in the 1930s by Iams and Salzberg⁹¹ and Zworykin⁹² at RCA and Kubetsky⁹³ in the former Soviet Union. The PMT

first demonstrated single-photon sensitivity very soon after these developments.^{94–96}

It was not until the work of McIntyre on Geiger-mode avalanche photodiodes (APDs) in the mid 1960s that the possibility of solid-state optical single-photon detection became a reality.⁹⁷ These APDs, when they are designed and fabricated specifically to operate as single-photon detectors rather than as analog detectors, are referred to as single-photon avalanche diodes (SPADs). Silicon-based SPADs enabled visible-photon counting with high efficiency and low noise (relative to analog semiconductor detectors).⁹⁸ However, SPAD development has been much more difficult in the infrared (IR), where the competing requirements of a material with good IR absorption and low-noise gain tend to be mutually exclusive. As a result, IR SPADs are inferior to Si SPADs in all characteristics, although there are significant efforts focused on addressing this problem.^{99–102}

The surge of research interest in the field of quantum information over the last few decades led to a concomitant surge in research into single-photon sources and single-photon detectors. This growth is clear from the citation-database search results shown in Fig. 1.

II. SINGLE-PHOTON SOURCES

A. Characteristics of an ideal single-photon source

An ideal single-photon source⁸⁶ would be one for which: a single photon can be emitted at any arbitrary time defined by the user (i.e., the source is deterministic, or “on-demand”), the probability of emitting a single photon is 100%, the probability of multiple-photon emission is 0%, subsequent emitted photons are indistinguishable, and the repetition rate is arbitrarily fast (limited only by the temporal duration of the single-photon pulses, perhaps). Deviations from these ideal characteristics, which are always present in real-world sources, must be considered when designing experiments. In Sec. II B, we consider deterministic single-photon sources based on color centers,^{103–105} quantum dots (QDs),^{106–108} single atoms,¹⁰⁹ single ions,¹¹⁰ single molecules,¹¹¹ and atomic ensembles,¹¹² all of which can to some degree emit single photons “on-demand.” In Sec. II C, we describe probabilistic single-photon sources. These sources rely on photons created in pairs via parametric downconversion (PDC) in bulk crystals^{113,114} and waveguides,¹¹⁵ and four-wave mixing (FWM) in optical fibers.^{116,117} For these sources the creation of photon pairs is probabilistic, rather than deterministic. However, because the photons are created in pairs, one photon (the heralding photon) can be used to herald the creation of the other photon (the heralded single photon). We would like to highlight here that while the distinction between a deterministic and a probabilistic source is clear in the abstract, that this distinction blurs in practice. An example of this is seen when a source classified as deterministic has loss in the extraction of the photon from the region where it is generated. As that emission (or extraction) loss increases, a theoretically deterministic source becomes more probabilistic in operation. Keeping this caveat in mind, these terms are helpful descriptors and thus we will use them.

TABLE I. Comparison of single-photon sources. Sources are characterized as probabilistic (P) or deterministic (D) (remembering the caveat that a deterministic source can in practice lose some or much of its determinism and operate in a more probabilistic fashion due to issues such as low emission efficiency). The wavelength range possible for each method is given, along with how far an individual source can be tuned. The inherent bandwidth indicates the typical spectral width of the emitted photons. The emission efficiency is the overall extraction efficiency of the source from generation of the photons to emission of the light, including any spectral filtering that would be necessary for typical quantum-information applications (the efficiency of a detector used to measure the source is not included). Note that for two-photon sources $g^{(2)}(0)$ typically increases as the generation rate increases, so the values here are for the lower end of the generation ranges.

Source type	Prob. or Deter.	Temp. (K)	Wave-length range general	Wave-length tunability specific	Inherent bandwidth	Emission efficiency	Output spatial mode	$g^{(2)}(0)$	Refs.
Faint laser	P	300	vis-IR	nm	GHz	1	Single	1	
Two photon (heralded)									
Atomic cascade	P	...	Atomic line	MHz	10 MHz	0.0001	Multi	...	122
PDC									
Bulk	P	300	vis-IR	nm	nm	0.6	Multi	0.0014	123–125
Periodically poled	P	300–400	vis-IR	nm	nm	0.85	Multi ^a	...	126
Waveguide (periodically poled)	P	300–400	vis-IR	nm	nm	0.07	Single	0.0007	127
Gated	D	300	vis-IR	nm	nm	0.27	Single	0.02	128, 129, 368
Multiplexed	D	300	vis-IR	nm	nm	0.1	Single	0.08	130
FWM									
DSF	P	4–300	IR	nm	nm	0.02	Single	...	131
BSMF	P	300	vis-IR	nm	nm	0.26	Single	0.022	132
PCF	P	300	vis-IR	10 nm	nm	0.18	Single	0.01	133
SOI waveguide	P	300	IR	10 nm	nm	0.17	Single	...	134
Laser-PDC hybrid	P	300	vis-IR	nm	nm	...	Single	0.37	120
Isolated system									
Single molecule	D	300	500–750 nm	30 nm	30 nm	0.04	Multi	0.09	135–137
Color center (NV)	D	300	640–800 nm	nm	nm	0.022	Multi	0.07	138
QD (GaN)	D	200	340–370 nm	nm	nm	...	Multi	0.4	106
QD (CdSe/ZnS)	D	300	500–900 nm	nm	15 nm	0.05	Multi	0.003	139
QD (InAs) in cavity	D	5	920–950 nm	10 GHz	1 GHz	0.1	Single	0.02	140
Single ion in cavity	D	≈ 0	Atomic line	MHz	5 MHz	0.08	Single	0.015	141
Single atom in cavity	D	≈ 0	Atomic line	MHz	10 MHz	0.05	Single	0.06	142, 143
Ensemble									
Rb, Cs	D	10^{-4}	Atomic line	MHz	10 MHz	0.2	Single	0.25	144, 145

^aWhile generally bulk and periodically poled PDC sources are inherently multimode, they can be engineered to emit with high overlap to a single-spatial mode (Ref. 146).

Section II D considers unique approaches to single-photon sources, including carbon nanotubes,^{118,119} quantum interference,¹²⁰ and two-photon absorption.¹²¹ In Table I, we list various types of single-photon sources and some relevant parameters with which to make comparisons and to get a feel for what is possible with each source type.

In Sec. IV, we discuss the importance of multi-photon emission to an application of quantum-information science, and the experimental status of single-photon sources for quantum-information protocols. Before moving on to discuss the current state-of-the-art in single-photon-source research, it is necessary to introduce a common tool for characterizing the single-photon nature of the emission of a source: the second-order correlation function.

By “single-photon nature” of the emission field of a source, we mean the probability of multiple-photon emission relative to the probability of single-photon emission. An ideal single-photon source would emit a single photon every time with zero probability of multiple-photon emission. A photon source can be characterized using the second-order correla-

tion function,^{147,148}

$$g^{(2)}(\vec{r}_1, \vec{r}_2, t_2 - t_1) = \frac{\langle : \hat{n}(\vec{r}_1, t_1) \hat{n}(\vec{r}_2, t_2) : \rangle}{\langle \hat{n}(\vec{r}_1, t_1) \rangle \langle \hat{n}(\vec{r}_2, t_2) \rangle}, \quad (1)$$

where \hat{n} denotes the photon-number operators $\hat{a}^\dagger \hat{a}$ and $::$ denotes operator normal ordering, i.e., with the annihilation operators \hat{a} to the right of the creation operators \hat{a}^\dagger . In many quantum optics experiments, a non-polarizing beamsplitter is used to divide the photon field into two equal parts, with each of them individually photo-detected. Such a setup is referred to as a Hanbury-Brown Twiss interferometer.¹⁴⁹ For an ideal single-photon emitter, the cross-correlation function for the two outputs of the beamsplitter is $g^{(2)}(0) = 0$ with $g^{(2)}(\tau) > g^{(2)}(0)$, because after emission of a single photon, the emitter must be excited again before a second photon can be emitted. It can never emit two photons at the same time. In practice, the time response of the detectors will determine minimum $g^{(2)}(0)$ that can be measured even with an ideal $g^{(2)}(0) = 0$ source. For comparison and completeness, an ideal laser is a source of photons where each emission is

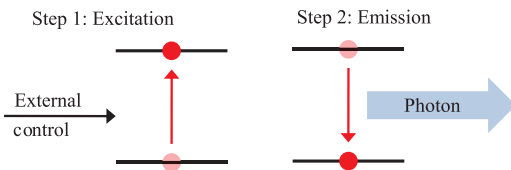


FIG. 2. (Color) Single emitter system excited by some means then emits a single photon.

independent of all other emission events and $g^{(2)}(\tau) = 1$ for $\tau = 0$ and for all τ . We note that in some applications, low multi-photon emission is the critical requirement rather than a low $g^{(2)}$ and thus an attenuated laser, due to its convenience, is often employed.

B. Deterministic sources

1. Single-emitter systems

There are a variety of systems that have been investigated for use as on-demand sources of single photons. Most of these are “single-emitter” quantum systems (shown idealistically in Fig. 2 with two internal levels), such as semiconductor quantum dots,^{106–108,150–153} mesoscopic quantum wells,¹⁵⁴ single molecules,^{111,155–157} single atoms,^{109,142,158} single ions,^{110,141,159} and color centers.^{103–105,160,161}

While each of these single-emitter approaches uses a different material system, most rely on similar principles of operation. When single-photon emission is desired, some external control is used to put the system into an excited state that will emit a single photon upon relaxation to some lower-energy state. Often coupling techniques using optical cavities are used to engineer the emission characteristics.

a. Single neutral atoms. Single-atom emitters are designed to work in the strong-coupling regime of cavity quantum electrodynamics, where the single photon profoundly impacts the dynamics of the atom-cavity system and the optical cavity greatly enhances single-photon emission into a single spatial mode with a Gaussian transverse profile. The operation of a single-atom emitter requires a tour-de-force experimental effort. To date, alkali atoms such as Cs and Rb have been used.^{109,143,158,162–164} Atoms are first captured and cooled inside a magneto-optical trap (MOT). After the MOT is turned off, the atoms fall freely under the pull of gravity. When atoms pass through a high-finesse optical cavity, an optical trap is turned on. For a single-atom emitter, it is important to have only one atom trapped inside the cavity. The atom has a Λ -type energy level system (or similar), consisting of two metastable ground states $|g\rangle$ and $|u\rangle$ and one excited state $|e\rangle$. The resonance of the optical cavity is made close to the transition of $|g\rangle \rightarrow |e\rangle$ and the transition of $|u\rangle \rightarrow |e\rangle$ is on-resonance with the pump laser pulse. The system consisting of the atom and the optical mode of the cavity (with state $|atomic\ state\rangle|photon\ number\rangle$) leads to a 3-level Hamiltonian system with states $|e\rangle|0\rangle$, $|u\rangle|0\rangle$, and $|g\rangle|1\rangle$.

With appropriate control of the pump laser pulse and atom-cavity coupling, the atomic state $|u\rangle$ can be coherently transferred to state $|g\rangle$ via stimulated Raman adiabatic pas-

sage (STIRAP).¹⁶⁵ During the process of STIRAP, a single photon is emitted in the cavity mode, which couples to the external field through one of the cavity mirrors. The atom-cavity mode is now in the state $|g\rangle|1\rangle$, which must be recycled to the state $|u\rangle|0\rangle$ for the next run of single-photon emission. The efficiency of single-photon generation for this approach can be close to unity (within an experimental uncertainty of 20%), although losses on exiting the system can be considerable, yielding in one example an emission probability of 4.8% with a $g^{(2)}(0) = 0.06$.¹⁴² The coherent process is reversible and the source can work both as a single-photon emitter and receiver and, because atoms are all identical, atom-based sources could be produced in quantity for a scalable system, although the experimental overhead would be formidable. Despite these advantages, single-atom emitters are compromised by a limited trapping time,¹⁴² fluctuating atom-cavity mode coupling¹⁶⁶ that can yield decoherence effects (although these effects can be made small), and possible multi-atom effects. All of these issues need to be resolved before single atoms can be used as true on-demand sources of single photons and nodes in quantum networks.

b. Single ions. Ions used as single-photon emitters^{110,141,167} also have a Λ -type energy-level configuration (i.e., with two ground states and one excited state). While both far-off-resonant Raman scattering and small-detuning (from resonance) STIRAP were proposed for single-photon generation, the Raman scattering path may offer higher single-photon emission probability.¹¹⁰ The use of a radio-frequency ion trap can stably localize the single ion in the center of the optical cavity, with the capability of confining the ion motion wavepacket to much smaller than the optical wavelength and fixing the wavepacket position with a precision of a few nanometers. This overcomes the issues encountered by single neutral-atom emitters and ensures continuous production of single-photon pulses. With only a single ion trapped inside the cavity, the possibility of multiple-photon events is eliminated.¹⁴¹ However, because the resonance transitions of ions are in the ultraviolet region, the excited states have strong spontaneous decay rates that compete with the emission of radiation into the cavity mode. In addition, the ion may remain in the ground state at the end of the excitation pulse without emitting a single photon. These factors can seriously reduce the probability of emitting a single photon during each pump cycle. As with single neutral atoms, single ions as the basis of a single-photon source have the advantage that they are all identical, and thus indistinguishability between different sources and different pulses from the same source is not an issue. In addition, achieving low levels of multi-photon emission and low decoherence do not seem to be inherent problems with ion-based systems. While significant progress has been made to manipulate several ions into a single system for quantum-information applications with separate areas for storage and processing^{168–170} (all important steps toward a truly scalable system), there are significant problems still to be faced. One such problem concerns how efficiently light can be collected, as the usual solution - using strong cavity coupling - is difficult with a charged particle.

c. Single molecules. Since the first observation of photon anti-bunching in a single-molecule system,^{156,171} single-photon emission by single molecules has been extensively studied by many groups in solid and liquid hosts, at both cryogenic and room temperatures. The molecular electron transition involved can be approximated by a 3-level system, which consists of a singlet ground state $|S_0\rangle$, a singlet excited state $|S_1\rangle$, and a triplet intermediate state $|T_1\rangle$. Each state represents a set of vibrational energy levels. An electron in a vibrational level of the ground state is optically transferred to a vibrational level in the excited state, and then radiatively de-excites back to the ground-state vibrational manifold. Thus the single-photon emission spans a broad spectrum. The single-photon emission repetitively occurs while the cycling of $|S_0\rangle \rightarrow |S_1\rangle \rightarrow |S_0\rangle$ continues, until the electron transitions to the dark state $|T_1\rangle$, which normally occurs with a small probability. Electrons staying in the dark state lower the emission rate of single photons and contribute to bunching on a longer time scale. This bunching at longer times is characteristic of any rapidly emitting light source that exhibits blinking.¹⁷² To emit a single photon on-demand, a pulsed pump laser can be used¹⁵⁷ with its pulse duration shorter than the lifetime of $|S_1\rangle$. An alternative approach is to apply a cw pump laser to the molecule, while sinusoidally sweeping an external electric field to shift the molecule's absorption line on and off the laser frequency through the Stark effect, thus periodically modulating the single-photon emission. The probability of single-photon emission approaches unity at high laser intensity. When implemented in free-space, the laser electric field with finite spatial extent may excite more than one molecule and contribute to multiple-photon events. Recent work with a single molecule inside a high finesse optical cavity shows better controllability of the single-photon emission field.¹¹¹ Despite this progress in emission control, a single molecule can become photo-bleached reducing its utility, but current advances in material development now allow hours of continuous operation of a single molecule under continuous illumination without bleaching. This approach needs further improvement for use in practical applications. So far single-molecule-based sources have only demonstrated relatively poor $g^{(2)}(0)$ values and photon indistinguishability between photons of the same molecule,¹⁷³ so it remains to be determined whether improvements can be made and different sources can be controlled so as to yield indistinguishable photons, necessary for scalable systems. We also note that while room temperature operation is possible,¹⁷⁴ tests of indistinguishability were performed at 1.4 K.¹⁷³

d. Quantum dots. Semiconductor quantum dots^{106,107,140,150–153,175–185} have been long studied for use as single-photon sources. They are created with methods such as molecular beam epitaxy, where the process of self-assembled (Stranski-Krastanov) growth¹⁸⁶ forms tiny islands of smaller-band-gap semiconductor embedded in a larger-band-gap semiconductor. In addition chemical synthesis can be used to produce colloidal quantum dots for single-photon source applications.¹³⁹ The small size of quantum dots results in a discrete energy structure for the electrons and holes. In the weak-excitation regime, an exciton (electron-hole pair) can be produced on demand.

Radiative recombination of the electron-hole pair results in single-photon emission. The radiative lifetime is on the order of 1 ns or less. Quantum dots can be excited either optically or electrically. Both optically and electrically excited QDs rely on there being a single system to limit emission to one photon at a time, but they do it via different physical paths. In the optical case, the excitation is created by photon absorption that saturates the single system. In the electrical case, the excitation is created by directly moving a charge carrier or carrier pair onto the QD. This can be done through the Coulomb blockade effect whereby charges can only move to the QD controllably one at a time. This has been referred to as an electron or photon turnstile.¹⁵⁴ Examples of optically active quantum dots include CdSe in ZnS,¹³⁹ InP in GaInP, and InAs in GaAs,¹⁸⁷ while an example of an electrically driven quantum dot is InAs.^{153,185}

The emission direction can be engineered by growing distributed-Bragg-reflection (DBR) mirrors on both sides of the quantum dots. Quantum dots can also be integrated into micro-cavities such as micro-pillar, disk, sphere, or photonic-crystal cavities.^{107,178,180,182–184} When the polarization and energy of the emission field are matched to the cavity, the rate of spontaneous emission of a quantum dot can be significantly increased due to the Purcell effect.¹⁸⁸ In addition, the well-defined cavity mode allows for collection of the emitted single photons into a single spatial mode. It is important to remember that while the generation quantum efficiency, i.e., the probability that an excitation creates a single photon, can be close to unity, the emission efficiency can still be low. Two electron-hole pairs can also be excited to form a biexciton state. In general, biexciton and exciton transitions differ in energy due to the local Coulomb interaction, but both biexciton and exciton transitions are doublets due to local crystal asymmetry. This effect can be used to generate polarization-entangled photon pairs.¹⁸⁹ Quantum dots as single-photon emitters need to operate at cryogenic temperatures, which is still technically cumbersome. In addition, the $g^{(2)}(0)$ levels achieved are not particularly low in comparison to other single-photon emitters, due to the fact that QDs live in an uncontrolled solid-state matrix. This, along with the fact that each QD is a unique structure, even though there is progress in tuning them controllably to make them appear indistinguishable,^{190,191} significantly dims the potential of practical scalable systems.

e. Color centers. A nitrogen-vacancy (NV) color center^{160,192} is formed by a substitutional nitrogen atom and a vacancy at an adjacent lattice position in diamond. The optical transition of NV centers can be modeled by a three-level energy system with ground state $|g\rangle$ and excited state $|e\rangle$, where $|e\rangle$ is also thermally coupled to a metastable state $|s\rangle$. The excited state can decay to the ground state $|g\rangle$ and emit a single photon. It can also thermally couple to the metastable $|s\rangle$. This state is referred to as a “shelving” state, as while in that state, the $|e\rangle$ to $|g\rangle$ emission ceases. The long lifetime of this shelving state $|s\rangle$ results in a decrease in the single-photon emission rate and also causes photon bunching when looking at longer times than the color center's main transition lifetime. When the nitrogen-vacancy center is used, the emission line is at 637 nm with a spectrum broader than 100 nm.^{160,192} When

another type of diamond lattice defect, the nickel-nitrogen-vacancy center is used, the zero-phonon emission line is around 800 nm and the spectral bandwidth is a few nanometers.^{103–105} We note that these are just two of hundreds of such color centers in diamond, so it is possible that other suitable defects may be of use in these applications.¹⁹³ Earlier studies with bulk diamond were restricted to low single-photon collection efficiency because of diamond’s high refractive index ($n = 2.4$), which leads to a small collection solid angle and spatial aberration. Now the use of diamond nanocrystals with a typical subwavelength size of 40 nm (Ref. 161) makes refraction irrelevant. It also reduces the collection of scattered background light, making the photon-antibunching effect more dominant, thus much more closely approximating an ideal single-photon source. Similar to single-molecule emitters, with efficient optical pumping, the radiative efficiency of a NV-center is close to unity at room temperature,¹⁶⁰ although some are operated at cryogenic temperatures. The lifetime of the excited state is a few nanoseconds. One important advantage of this implementation is that NV centers are photostable and do not exhibit bleaching or photo-blinking. NV centers with $g^{(2)}(0)$ values less than 0.1 have been reported.¹³⁸ A disadvantage of NV centers is that they are not identical, although some tunability has now been demonstrated via external electric fields.¹⁹⁴ There are also efforts to build optical cavities near them¹⁹⁵ improving coupling efficiency and offering a potential path to scalability.

2. Ensemble-based systems

In addition to these single-emitter approaches, on-demand single-photon sources have also been realized that use collective excitations in ensembles of atoms.^{144,145,196,197} These atoms have “ Λ ”-type energy levels (or similar), consisting of two metastable ground states $|g\rangle$, and $|u\rangle$, and one excited state $|e\rangle$ as seen in Fig. 3. All atoms are first optically pumped to, for example, state $|u\rangle$. Then the ensemble is illuminated with a weak “write” laser pulse defined by its frequency and momentum (ω_w, \vec{k}_w), which couples to the $|u\rangle \rightarrow |e\rangle$ transition to induce the emission of photons (ω_s, \vec{k}_s) on the $|e\rangle \rightarrow |g\rangle$ transition with a small probability. The loose boundary condition allows these Raman photons to be spontaneously emitted in multiple spatial modes. The successful detection of a single Raman photon within a particular acceptance solid angle projects the whole ensemble into a specific single spin-wave state ($\vec{k}_{spin} = \vec{k}_w - \vec{k}_s$) due to energy and momentum conservation. The successful detection of two Raman photons within the same acceptance solid angle projects the whole ensemble into a specific spin wave state with two quanta (assuming unit detection efficiency), and so on for higher numbers of excitations.

When the excited atomic ensemble is illuminated by a “read” laser pulse (ω_r, \vec{k}_r) which resonantly couples to the $|g\rangle \rightarrow |e\rangle$ transition, the atomic spin wave excitations are mapped onto photon modes (ω_i, \vec{k}_i) on the $|e\rangle \rightarrow |u\rangle$ transition. To operate as a single-photon source, a pair of acceptance solid angles needs to be carefully chosen to satisfy the momentum conservation ($\vec{k}_w - \vec{k}_s = \vec{k}_{spin} = -(\vec{k}_r - \vec{k}_i)$).

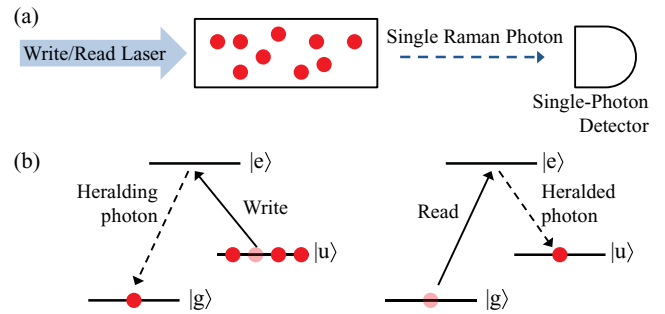


FIG. 3. (Color online) Ensemble-based emitter scheme (a). Laser pulses first prepare the system in state $|u\rangle$, then probabilistically create a single collective excitation (b). The successful excitation is heralded by the detection of a single emitted photon at the $|e\rangle \rightarrow |g\rangle$ transition. Then a strong read pulse deterministically pumps the single excitation back to its original state generating just a single photon at the $|e\rangle \rightarrow |u\rangle$ transition.

The “write” laser pulse is made weak to reduce the likelihood of creating more than one photon-atomic-spin-wave excitation in the selected mode. (Because detection efficiency is less than unity and typically not photon-number resolving, the detection cannot distinguish between one and more than one excitation).

In many experiments, the major decoherence mechanism is related to atomic motion, i.e., the atoms may move out of the interaction region, (the typical transverse dimension of the interaction region of laser-atomic ensemble in experiments is 100 μm), or the atomic motion perturbs the phase of the excited atomic spin wave which destroys the momentum conservation, so even though the photon is stored it will not be retrieved in the anticipated mode. The first problem may be overcome by using optical-dipole trapping or an optical lattice. The second type of dephasing mechanism is reduced by choosing a smaller angle with respect to the optical axis of the write and read pulses for collecting the single photons. A smaller angle corresponds to a longer atomic spin wavelength ($\lambda_{spin} = 2\pi/k_{spin}$) that is more resistant to motion-induced phase perturbation, resulting in longer coherence times which better allows for user-defined programmable delays. Since the first experimental demonstrations of an on-demand single-photon source based on atomic ensembles of Cs and Rb seven years ago, the demonstrated spin-wave coherence time has been extended from a few hundred nanoseconds to one millisecond.^{198,199}

C. Probabilistic sources

Although many applications, especially those in the field of quantum-information science, require an on-demand source of single photons, and this has led to intense research into developing truly deterministic single-photon sources as described in Sec. II B, there is another approach. This approach is to generate correlated pairs of photons, where the detection of one photon (the heralding photon, or sometimes referred to as the conditioning photon) of the pair “heralds” the existence of the other photon (the heralded single photon). Typically such “heralded single-photon sources” involve a laser excitation of a nonlinear optical material.

Although this type of source is not “on demand” because the pair production is a probabilistic process, the fact that the photons emitted are heralded is of much use for many quantum information applications.

Because of the statistical nature of the pair production process, these heralded sources must be held to average pair production levels much less than one to avoid producing multiple pairs which would result in the heralded channel containing more than one photon. If a pair is created, it will be created at the time of one of the excitation pulses, and it will be heralded by the detection of one of the two photons. Of course, losses in the heralded path will result in some heralded photons not being emitted from the source. In addition, false heralds due to dark counts and stray light will not yield heralded photons. And finally, losses in the heralding channel will result in unheralded photons being emitted from the source, which can be a problem in some applications. As suggested by Klyshko,⁷² this last issue can be ameliorated somewhat through the use of a shutter on the heralded channel that only opens when triggered by a herald.^{128, 129, 368}

1. Parametric downconversion

Although initial efforts with photon-pair sources employed atomic-cascade schemes,²⁰⁰ over the last two decades the most relied on schemes for creating correlated photon pairs have used spontaneous parametric downconversion (PDC). This pair production process was predicted theoretically by Louisell *et al.* in 1961 (Ref. 201) and its use as a source of nonclassical light was first proposed by Zeldovich and Klyshko in 1969 (Ref. 202) with pair correlations first observed in 1970 (Ref. 203).

In PDC, a pump laser illuminates a material with a $\chi^{(2)}$ optical nonlinearity, creating two photons under the constraints of momentum and energy conservation (Fig. 4). The energy and momentum conservation constraints determine the possible wavevector relations between the two down-converted photons, a constraint generally referred to as phase matching (for a general introduction to PDC, see Refs. 204 and 205). This constraint presents both an advantage and a limitation. It is useful in that the emission from these sources is highly directional, which is an advantage in most applications. It is a drawback in that the inherent dispersion of transparent material is generally not controllable other than the very limited control offered by temperature. As a re-

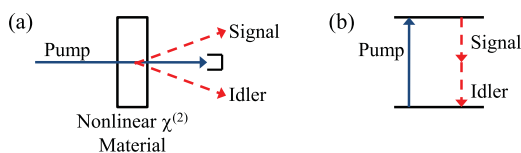


FIG. 4. (Color online) (a) Parametric downconversion of one input photon converted to two output photons. (Conversion efficiencies of a pump photon into a photon pair can be 10^{-6} (Ref. 213), so care must be taken to reject the bulk of the pump light). Momentum conservation governs the emission angles. While a noncollinear emission geometry is shown, a collinear geometry can and often is used by orienting the optic axis angle appropriately. (b) The conversion process is nonresonant so that a wide range of wavelengths can be created subject only to energy and momentum conservation.

sult the phase-matching constraints often cannot be met for the particular wavelengths of interest. This limitation can be surmounted by techniques whereby different refractive indices can be selected or an effective index can be controlled. The former relies on polarization birefringence and the latter on waveguide design that impacts propagation velocities in a structure. There are different types of polarization phase matching possible for parametric downconversion: type-I, where the two photons have the same polarization, and type-II, where the two photons have orthogonal polarization. In addition, a type-0 phase matching, with all polarizations aligned, is possible in appropriately engineered media.²⁰⁶ There are many properties of the down-converted photon pairs that can be correlated, including time, energy, momentum, polarization, and angular momentum for use in making a heralded single-photon source.

The $\chi^{(2)}$ nonlinearity required for parametric downconversion occurs in many different inorganic crystals, including, for example, KD*P (potassium dideuterium phosphate, KD_2PO_4), BBO (beta barium borate, BaB_2O_4), LiNbO_3 (lithium niobate), and LiIO_3 (lithium iodate). Materials are typically chosen for the strength of the $\chi^{(2)}$ nonlinearity, as well as whether the phase-matching constraints can be satisfied for the output and pump wavelengths of interest.

As mentioned above, researchers are also investigating how to engineer crystals with the wavelength and phase-matching properties they desire. The most promising of these techniques is referred to as “periodic poling” which involves periodically changing the sign of the crystal nonlinearity to achieve phase matching where it is otherwise impossible,²⁰⁷ thus allowing useful down-conversion efficiency. This expansion of options benefits other optimizations, such as improving the degree of factorability of the states produced (that is states without spectral correlation between the signal and idler photons, an important characteristic when indistinguishability or entanglement is required).^{208–211} For a non-factorable state, detection of the heralding photon collapses the state of the heralded photon in a way that can be different from one pair to the next. With factorable states, the characteristics of the heralded photon are completely independent of the measurement result obtained upon detection of the heralding photon. To date, many experiments have demonstrated the usefulness of periodic poling,^{212–215} with a recent source demonstration focused on high degree of factorability.¹⁴⁶ In addition to these schemes for developing factorable states as a means to improve efficiency and purity in some applications, a recent result has shown that equivalent results may be achieved by relying on temporally resolving single-mode detection rather than direct spectral filtering.²¹⁶

One disadvantage of $\chi^{(2)}$ -based downconversion in crystals is the spatial mode of the photon pairs. The photon pairs are typically created in multi-mode cones surrounding the pump laser, making efficient collection by single-mode fibers difficult. In part to circumvent this problem, recent research has focused on producing correlated photon pairs directly in a single-mode waveguide. This constrains the pairs produced to just a single or a few spatial modes, as well as controlling the phasematching through the impact of the waveguide

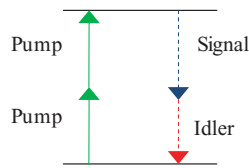


FIG. 5. (Color) Four-wave mixing, where two input photons are converted to two output photons. Equal input energy pump photons are shown creating a nondegenerate pair of output photons, but some applications make use of the reverse process with nondegenerate pump photons producing degenerate output photons. Also because of the nonlinearity is typically lower than in PDC a longer interaction length is required, such as can be obtained in an optical fiber. Such a medium necessarily requires a collinear geometry although higher nonlinearity media such as atomic vapor can overcome this restriction.

dimensions on the dispersion,^{217,218} and improving the degree of factorability of the resulting states, as just discussed.²¹⁹

2. Four-wave mixing

Four-wave mixing, a $\chi^{(3)}$ nonlinear process in which two pump photons are converted into two correlated photons (Fig. 5), is the dominant nonlinear process in centrosymmetric materials such as glass that do not allow $\chi^{(2)}$ nonlinearity. Even though the absolute $\chi^{(3)}$ nonlinearity of glass is very small, optical fiber with its long interaction length can be used to produce photon pairs via FWM. To date, many experiments have demonstrated generation of correlated photon pairs in a single spatial mode using four-wave mixing in single-mode optical fibers,^{220–226} with recent results demonstrating heralded single-photon sources using dispersion shifted fiber (DSF), photonic crystal fiber (PCF),¹¹⁷ birefringent single-mode fiber (BSMF),¹³² and Silicon-on-insulator (SOI) waveguides.^{134,227–229} One issue with pair sources based on FWM is that Raman scattering produces a single-photon background that must be either suppressed or avoided.^{131,223,230,231}

3. Probabilistic source issues

One disadvantage of heralded single-photon sources based on probabilistic correlated photon generation, such as the PDC- and FWM-based sources just discussed, is that there exists a nonzero probability of generating more than one pair of photons, and this multiple-pair probability increases together with the probability of generating one pair. Since typical SPADs cannot distinguish the detection of one photon from the simultaneous detection of more than one photon, multiple-pair generation cannot be distinguished from single-pair generation. As a result, photon-pair sources must be operated so that the probability of generating a single pair is low (typically $P \approx 10\%$). In this sense, the $g^{(2)}(0)$ of these sources inherently degrades as P increases.²³² Other effects such as background scattering only degrade (increase) the $g^{(2)}(0)$. Solutions to this scaling problem based on multiplexed photon-pair source arrangements have been proposed that allow the single-pair emission probability to increase without increasing the multiple-pair emission probability,^{233–236} and while

full experimental realizations of these schemes have not yet been implemented, progress is being made.¹³⁰ We note also that such a multiplexed source scheme moves a probabilistic heralded source toward more deterministic operation as the single-photon emission becomes more frequent. Photon-number resolving detectors (see Sec. III C) also help with this multi-photon emission problem by allowing the discrimination between single-pair and multiple-pair emission events.

Another way of dealing with the problem of probabilistic emission in these sources is to couple the heralded source with a photon storage mechanism, where once heralded a photon is stored until needed. This moves the probabilistic pair source toward deterministic operation. Such schemes require efficient coherent exchange of the photon state to the stored state and back, and long-lived storage. In addition, the memory storage and retrieval times must be fast enough for practical operation. While storage for photons is challenging, a number of schemes have been proposed and implemented to varying degrees.^{237–241}

In addition to being used as a heralded single-photon source, correlated photon-pair emission, whether from parametric downconversion or four-wave mixing, can also be used for the metrology application of calibrating single-photon detectors.^{76,78,80} Finally as with PDC, there are efforts to create output photon-pair states with a high degree of factorability by dispersion engineering through the geometry of the fiber.²⁴²

D. Nontraditional approaches to single-photon sources

Other approaches to single-photon sources are also being pursued that are at an earlier stage of development than the sources previously discussed. Examples include sources that use carbon nanotubes,^{118,119} quantum interference,¹²⁰ and two-photon absorption.¹²¹

Hoge *et al.*¹¹⁹ investigated the photoluminescence of single carbon nanotubes at low temperatures. A phonon sideband of the nanotube was excited by a femtosecond pulsed laser 70 meV above the peak emission energy. By directing the photo-luminescence to a Hanbury-Brown-Twiss setup, the second-order correlation function at zero time delay was measured to be $g^{(2)}(0) = 0.03$ at 4.2 K (with a peak emission wavelength of ≈ 855 nm), demonstrating that the nanotube only very rarely emits more than one photon upon excitation.¹¹⁹

A different approach has been used recently to demonstrate entanglement generation and a single-photon source based on quantum interference.^{120,243,244} The idea is to interfere a weak coherent state with a pair of photons produced via parametric downconversion on a 50-50 beamsplitter. By properly adjusting the relative phases and amplitudes of the coherent state's two-photon probability amplitude and the two-photon probability amplitude from the downconversion process, these two terms can be made to interfere destructively so that the probability of detecting two photons in the output beam is suppressed. This essentially creates a modified coherent state that ideally has no two-photon term. The

experiments of Pittman *et al.*¹²⁰ use a Hanbury-Brown-Twiss-type setup to demonstrate a suppression of the two-photon probability by a factor of about 2.7, corresponding to a $g^{(2)}(0)$ of ≈ 0.37 .

Finally, Jacobs, *et al.*¹²¹ have proposed a scheme for making a heralded single-photon source using laser pulses and two-photon absorption. In this scheme, two separate laser pulses are each sent into a two-photon absorbing medium, transforming each pulse into a field with equal probabilities of having zero or one photon, and arbitrarily small multi-photon probability. These two pulses are then sent to a “controlled-not Zeno gate” which itself uses a two-photon absorbing medium. The operation of this gate is such that if a photon is detected in one of the gate’s output fields, then the other output contains a single photon. In this way, a heralded single-photon source is produced. For this scheme to be demonstrated in the lab, a suitable two-photon absorbing medium must be found.

III. SINGLE-PHOTON DETECTORS

A. Characteristics of an ideal single-photon detector

We consider an ideal single-photon detector to be one for which: the detection efficiency (the probability that a photon incident upon the detector is successfully detected) is 100%, the dark-count rate (rate of detector output pulses in the absence of any incident photons) is zero, the dead time (time after a photon-detection event during which the detector is incapable of detecting a photon) is zero, and the timing jitter (variation from event to event in the delay between the input of the optical signal and the output of the electrical signal) is zero. In addition, an ideal single-photon detector would have the ability to distinguish the number of photons in an incident pulse (referred to as “photon-number resolution”); many single-photon detectors (e.g., single-photon avalanche photodiodes, photomultiplier tubes (PMT), superconducting nanowire single-photon detectors (SNSPD)) as typically used are not photon-number resolving and can only distinguish between zero photons and more than zero photons. Deviations from these ideals negatively impact experiments in varying ways depending on the detector characteristic and measurement involved.²⁴⁵

We consider in Sec. III B the details of various approaches to non-photon-number-resolving single-photon detectors, including the single-photon avalanche photodiode²⁴⁶ (InGaAs,^{101,247–249} Ge,²⁵⁰ and Si;²⁵¹), quantum dot,²⁵² superconducting nanowire,²⁵³ and up-conversion detectors.^{254–256}

In Sec. III C we consider photon-number resolving detectors such as the transition-edge sensor (TES),²⁵⁷ superconducting-tunnel-junction (STJ) detector,^{258–261} parallel superconducting nanowire single-photon detector (P-SNSPD),²⁶² charge-integration photon detector (CIPD),²⁶³ visible-light photon counter (VLPC),^{113,264} quantum-dot optically gated field-effect transistor (QDOGFET),²⁶⁵ time-multiplexed SPAD,²⁶⁶ SPAD array, and the recently reported number-resolving capability of a detector based on a single SPAD.²⁶⁷ The characteristics of examples of many of these detectors are compiled in Table II for ease of comparison.

There is not always a clear distinction between photon-number-resolving and non-photon-number-resolving detectors, as some detectors considered to be non-photon-number-resolving do in fact have some degree of photon-number-resolving capability, and there are ongoing efforts to add or improve number-resolving capability to those detectors without it. Conversely, even those detectors classified as photon-number-resolving do not tell the true number of incident photons if their efficiency is less than unity. In addition, dark counts add to the discrepancy between the measured result and the true incident photon number.

Section III D discusses unique approaches to single-photon detection, such as cryogenic thermoelectric detectors (QVDs),²⁶⁸ a proposal for a potentially very high efficiency single-photon number-resolving detector with an atomic vapor absorber,²⁶⁹ and a proposal for a quantum nondemolition single-photon number-resolving detector that uses giant Kerr nonlinearities.²⁷⁰

Almost all single-photon detectors involve the conversion of a photon into an electrical signal of some sort. It is the job of the detector electronics to ensure that each photo-generated electrical signal is detected with high efficiency. Additional electronics is often required after detection to return the detector as quickly as possible back to a state that allows it to detect another photon. The electronics is often as important as the detector itself in achieving the ideal characteristics outlined above. Section III E discusses various aspects of detector electronics.

As mentioned, one of the fields currently driving much of the research toward improved single-photon-detector technology is quantum-information science. In particular, the security and performance of many quantum-communication protocols depend strongly on detector properties such as detection efficiency. In Sec. IV, we discuss the importance of various source and detector properties to applications in the field of quantum-information science.

B. Non-photon-number-resolving detectors

Non-photon-number-resolving detectors are the most commonly used single-photon detectors. While detecting a single photon is a difficult task, discriminating the number of incident photons is even more difficult. Because the energy of a single photon is so small ($\approx 10^{-19}$ J), its detection requires very high gain and low noise. In many detectors this is achieved by converting the incoming photon into a charge carrier and then using a high voltage avalanche process to convert that single charge into a macroscopic current pulse.

1. Photomultiplier tube

In the original visible-photon-counting detector, a PMT, (Fig. 6) a photon knocks an electron out of a photocathode made of a low workfunction material. That electron is accelerated to the first dynode where it knocks out more electrons. The process repeats as those electrons are accelerated to each subsequent dynode until typically a pulse of 10^6 electrons are generated, which can then be detected by ordinary

TABLE II. Comparison of single-photon detectors based on a table from Ref. 309 using a figure of merit given by the ratio of the detection efficiency to the product of the dark-count rate and the time resolution (assumed to be the timing jitter), $\eta/(D\delta t)$. Maximum count rate is a rough estimate from the the detector's output pulse width or count rate that yields 100% dead time. The photon-number-resolving (PNR) capability is defined here as: none) for devices that are typically operated as a photon or no photon device, some) for devices that are made from multiple detectors that individually have no PNR capability and thus are limited in the photon number that can be resolved to the number of individual detectors, and full) for devices whose output is inherently proportional to the number of photons even if their proportional response ultimately saturates at high photon levels.

Detector type	Operation temperature (K)	Detection efficiency, wavelength $\eta(\%)$, λ (nm)	Timing jitter, δt (ns) (FWHM)	Dark-count rate, D (ungated) (1/s)	Figure of merit	Max. count rate ($10^6/s$)	PNR capability	Refs.
PMT (visible–near-infrared)	300	40 @ 500	0.3	100	1.3×10^7	10	Some	271,272
PMT (infrared)	200	2 @ 1550	0.3	200 000	3.3×10^2	10	Some	273
Si SPAD (thick junction)	250	65 @ 650	0.4	25	6.5×10^7	10	None	274
Si SPAD (shallow junction)	250	49 @ 550	0.035	25	5.6×10^8	10	None	275
Si SPAD (self-differencing)	250	74 @ 600	...	2000	...	16	Some	276
Si SPAD (linear mode)	78	56 @ 450	...	0.0008	...	0.01	Full ^a	277
Si SPAD (cavity)	78	42 @ 780	0.035	3500	3.4×10^6	10	None	278
Si SPAD (multipixel)	290	40 @ 532	0.3	25 000–500 000	1×10^4	30	Some	279,280
Hybrid PMT (PMT + APD)	270	30 @ 1064	0.2	30 000	5×10^4	200	None	281,282
Time multiplexed (Si SPAD)	250	39 @ 680	0.4	200	5×10^6	0.5	Some	234
Time multiplexed (Si SPAD)	250	50 @ 825	0.5	150	7×10^6	2	Some	283
Space multiplexed (InGaAs SPAD)	250	33 @ 1060	0.133	160 000 000	1.6×10^1	10	Some	284
Space multiplexed (InGaAs SPAD)	250	2 @ 1550	0.3	None	285
InGaAs SPAD (gated)	200	10 @ 1550	0.370	91	3.0×10^5	0.01	None	286
InGaAs SPAD (self-differencing)	240	10 @ 1550	0.055	16 000	1.1×10^5	100	None	287
InGaAs SPAD (self-differencing)	240	10 @ 1550	Full	267
InGaAs SPAD (discharge pulse counting)	243	7 @ 1550	...	40 000	...	10	None	288
InP NFAD (monolithic negative feedback)	243	6 @ 1550	0.4	28 000	5×10^3	10	Some	289,290
InGaAs (self-quenching and self-recovery)	300	... @ 1550	10	...	–	3	Some	291
CIPD (InGaAs)	4.2	80 @ 1310	0.001	Full	263
Frequency up-conversion	300	8.8 @ 1550	0.4	13000	1.7×10^4	10	None	292
Frequency up-conversion	300	56-59 @ 1550	...	460000	...	5	None	254,293
Frequency up-conversion	300	20 @ 1306	0.62	2200	1.5×10^5	10	None	294
VLPC	7	88 @ 694	40	20000	1.1×10^3	10	Some	295
VLPC	7	40 @ 633	0.24	25000	6.7×10^4	10	Some	296
SSPM	6	76 @ 702	3.5	7000	3×10^4	30	Full	297
TES(W)	0.1	50 @ 1550	100	3	1.7×10^6	0.1	Full	298
TES(W)	0.1	95 @ 1556	100	0.1	Full	299
TES(Ha)	0.1	85 @ 850	100	0.1	Full	300
TES (Ti)	0.1	81–98 @ 850	100	1	Full	301–303
SNSPD	3	0.7 @ 1550	0.06	10	1.2×10^7	100	None	304
SNSPD (in cavity)	1.5	57 @ 1550	0.03	1000	None	253
Parallel SNSPD	2	2 @ 1300	0.05	0.15	2.7×10^9	1000	Some	262
STJ	0.4	45 @ 350	2000	0.01	Full	258,259,305
QD (resonant tunnel diode)	4	12 @ 550	150	0.002	4×10^9	0.25	Full	306
QDOGFET (field-effect transistor)	4	2 @ 805	10000	150	10	0.05	Full	265,307,308

^aPNR should be possible, but none has been demonstrated as of yet.

electronics. All this requires operation in vacuum. While we have put the PMT in the section with non-photon-number-resolving detectors, some models have low enough gain noise to make it possible to partially resolve output pulses resulting from different numbers of incoming photons, with the first such demonstration made by incorporating a first dynode specially prepared to yield higher electron emission.^{310,311} We also note that a PMT can be used as an n-photon detector for wavelengths with energies below the bandgap so that more than one photon is needed to generate a photoelectron, albeit with greatly reduced detection efficiency and requiring tightly focused beams to enhance the multi-photon absorption process.³¹²

The efficiency of PMTs is typically in the range of 10% to 40%, limited by the efficiency with which the incoming photon knocks out the initial photoelectron from the photosensitive surface (the photocathode). While these efficiencies are impressive for a pioneering technology, they fall short of the requirements of many modern applications. Other features of PMTs are the large sensitive areas (cm^2 or even up to m^2), fast response (low timing jitter and low dead time) with the capability to resolve photons separated by a nanosecond, and the low level of dark counts (output pulses that result from causes other than incident photons). The dark-count rates can be as low as a few events per second, particularly if the PMT is cooled by a few tens of degrees C. Their major drawbacks

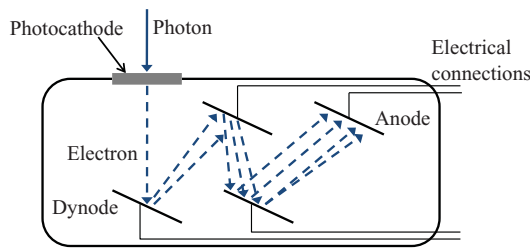


FIG. 6. (Color online) A photomultiplier, the first detector able to sense a single optical photon, is shown schematically with a transmissive photocathode and just 3 dynodes. The photocathode may be designed to have the photoelectrons emitted from its front or back surface and typically 10 dynodes are used.

include their reliance on vacuum tube technology which limits their lifetime, reliability, and scalability.

2. Single-photon avalanche photodiode

The SPAD (Fig. 7) uses a similar process to the PMT, but the initial photon absorption creates an electron-hole pair and the charge multiplication is continuous, with a voltage applied across a semiconductor lattice rather than between discrete dynodes suspended in vacuum. SPADs are typically run in what is referred to as “Geiger-mode,” where a bias voltage greater than the diode’s breakdown voltage is applied. Thus when a charge is generated by an incoming photon, the charge multiplication (or avalanche) proceeds until it saturates at a current typically limited by an external circuit, and that current is self-sustaining. The saturated avalanche current must be terminated by lowering the bias voltage below the breakdown voltage before the SPAD can respond to a subsequent incoming optical pulse. This saturation means that gain in Geiger mode is not a useful concept. Geiger-mode SPADs can have detection efficiencies higher than PMTs, up to 85% (for Si SPADs in the visible), although SPAD dark-count rates and timing jitter are somewhat higher than the best PMTs and for IR SPADs, efficiencies are in the 10% to 20% range with dark-count rates much higher than PMTs.^{247,250} To reduce dark-count rates, SPADs are typically cooled with thermoelectric coolers to temperatures of 210 K to 250 K.

In addition, the SPAD gain medium typically has trap sites that must be allowed time to depopulate after an

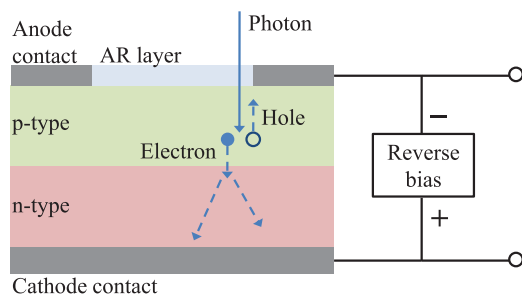


FIG. 7. (Color) A single-photon avalanche photodiode is shown with distinct regions for the photo-absorption and carrier multiplication processes. The voltage is applied to accelerate the electrons toward the multiplication region. A front-illuminated geometry with an antireflection (AR) coating to improve efficiency is illustrated, but back-illuminated designs are also used.

avalanche has occurred and before the bias voltage can be restored. If those sites are not allowed to depopulate, a second avalanche can be initiated by carriers released from traps rather than from a new photon. This “afterpulsing” effect necessitates additional waiting time after a pulse before rebiasing the device. As a result, SPAD dead times can range from tens of nanoseconds to 10 μ s. This is a particular problem for SPADs designed for IR sensitivity.

There are a number of schemes focused on these issues to reduce dead time or its effect,²⁸⁵ to reduce afterpulsing (e.g., by detection multiplexing to maximize the time recovery between firings of a single detector²⁸⁵ and by self-differencing of adjacent pulses to reduce avalanche currents and output transients relative to the avalanche signal of interest²⁴⁹), to improve IR performance, and to realize some photon-number-resolution capability. Efforts toward photon-number-resolution are discussed in Sec. III C. Some design techniques can result in very low time-jitter detectors. These usually involve thinner absorption regions so there can be a tradeoff between detection efficiency and timing jitter, although there is an effort to regain some efficiency by using cavity enhancement around the thinner absorber.²⁷⁸ An in-depth look at the details of this type of tradeoff can be found in Ref. 313 and a commercial example of this tradeoff can be seen in Ref. 275.

While all commercial SPADs operate in Geiger-mode, there are efforts to develop linear-mode operation for photon counting. This would have the advantages of having an output that is proportional to the number of incident photons, yielding photon-number resolution, lower afterpulsing due to lower current flow and less trap filling, and reduced dead time. The smaller current pulses generated in the linear mode require long measurement times to reduce the readout noise and thus in one recent demonstration a 56% detection efficiency and 0.0008 /s dark-count rate was achieved, but at a 10 kHz maximum repetition rate.²⁷⁷ While these linear devices can in principle provide photon-number resolution, the noise on the gain and the smaller signals involved can broaden the output current pulse amplitudes so much that pulses due to different numbers of incident photons cannot be resolved. We are unaware of any demonstrated number resolution of these devices.

Having just described PMT and SPAD detectors, we note that there is a detector that is essentially a hybrid between the two. It consists of a photocathode and electron impact multiplication stage in vacuum providing gain $\approx 10^3$ followed by an avalanche diode multiplication region for a total gain above 10^4 . This arrangement allows for a photocathode optimized for a particularly difficult wavelength for photon counting detectors, 1060 nm, with efficiency of 30% and a low dark-count rate of 30 000 counts/s.^{281,282}

3. Quantum-dot field-effect transistor-based detector

A quantum dot in conjunction with a field-effect transistor (FET) has been reported to offer single-photon sensitivity in the near IR. This detector design, sometimes referred to as a QDOGFET,^{265,307,308} consists of an optical absorber with a thin layer of quantum dots between

the gate electrode and conduction channel in an FET. The photo-generated charges move to the quantum dots where they are trapped. Those trapped charges shield the gate potential and thus modify the channel conductance of the FET. In one implementation, the trapped carriers are holes that reduce the negative field of the quantum dots allowing the conductivity to increase.¹⁷⁵ Thus current can flow unimpeded until the photon-generated carrier is removed or recombines, yielding an observable single-photon signal. We also note a detector that operates on the same scheme as the QDOGFET but instead uses native traps, rather than quantum dots, to store the photo-generated charges.³¹⁴

Another quantum dot-based approach uses the photo-generated carriers to enhance resonant tunneling through a double barrier. By adjusting the field so that the well between the two barriers matches the energy of the band on the other side of one of the barriers, the tunneling rate increases dramatically and in proportion to the number of incident photons. In this scheme the photo-generated holes trapped by the quantum dots provide the field necessary to shift that intermediate band into resonance.³⁰⁶ We note a detector that works on a similar principle but because it operates in the far IR it is beyond the scope of this review.²⁵²

4. Superconducting nanowire single-photon detector

This fast (timing jitter <50 ps) single-photon detector relies on a narrow superconducting wire that is biased with a current at a level just below the critical current density, above which the wire must revert to normal resistance^{253,315–317} (Fig. 8). In this state, when an incoming photon is absorbed, its energy causes a small spot of the wire to go normal. This in turn causes the current to flow around the normal resistance region and as a result the current density is increased in those adjacent regions. Those adjacent regions now exceed the critical current density and a normal resistance region is formed all the way across the width of the wire. This small normal region of the superconducting wire yields a voltage spike that indicates the detection of a single photon. Because this detection mechanism requires a very narrow wire (≈ 100 nm), a meandering surface-filling arrangement of the wire is used to create a practical sensitive area. In addition, devices fabricated with a mirror on top of the nanowire meander made of NbN, thus forming an optical cavity have achieved detection efficiencies in the neighborhood of 25%.^{318,319} In these devices the light first passes through the NbN substrate subject to reflective losses. Subsequent devices have achieved efficiencies (not including light missing the detector active area) of 57% and 67% at 1550 nm and 1064 nm respectively,²⁵³ by adding an antireflection coating to the input side of the cavity device. These detectors do not suffer afterpulsing, although they can latch³²⁰ into a mode where they stay in the normal state due to self-heating of the normal region and have to be actively reset by reducing the current flow. Because these detectors require superconductivity, their operating temperatures are typically in the range of 4 K or less.

While the arrangement just described cannot discriminate between one or more incident photons, as we shall see in

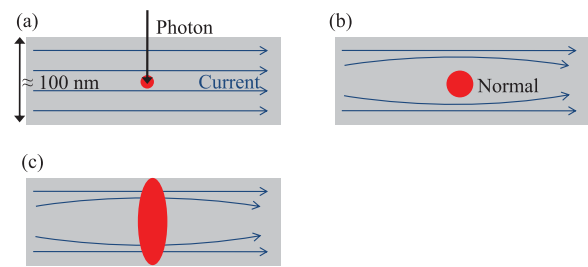


FIG. 8. (Color online) A section of a superconducting nanowire single-photon detector is shown with a bias current just below the critical current density that would drive the wire normal. (a) An incoming photon creates a small normal region within the nanowire. (b) The superconducting current is expelled from the normal region, increasing the current density in the adjacent areas of the nanowire. (c) That increase in current density is enough to drive those adjacent regions normal, which in turn results in a measurable voltage drop across the detector.

Sec. III C 3 there are efforts to provide this detector with some photon-number-resolving capability.^{262,319}

5. Up-conversion single-photon detector

Up-conversion of a photon from the infrared, where detector characteristics are typically poor, to the visible spectral region, where detector performance is better, has been demonstrated by a number of research groups³²¹ and has been commercialized.^{272,322} The scheme uses sum-frequency generation in a nonlinear crystal, where a strong pump beam mixes with the IR single photon of interest to create a single photon at the sum frequency in the visible. Both visible SPADs and PMTs have been used for the detection of the up-converted photon. The key drivers for these efforts are better detection efficiency at low dark-count rates, and higher count rates with better pulse-pair resolution. The overall efficiency of this approach is the product of the optical conversion efficiency, the optical losses throughout the system, and the visible detector efficiency. The up-conversion step has been demonstrated with near unit efficiency,²⁹³ with the other factors limiting the overall efficiency to 56% to 59% to date.^{254,293,321,323} Background count rates are also of concern as the up-conversion process can produce a significant number of unwanted photons. To address this, having the up-conversion pump photon at an energy lower than the IR photon to be up-converted rather than the other way around, may prove advantageous in some applications.²⁹⁴ This avoids having the pump beam create Raman photons at the wavelength of interest that are then up-converted as if they were incident IR photons.

C. Photon-number-resolving detectors

Developing photon-number-resolving (PNR) detectors is important for many applications in quantum-information science, such as quantum computation using linear optics³²⁴ and quantum communication.¹⁵ Section IV describes how photon-number resolution impacts quantum communication protocols.

One direct approach to gaining photon-number-resolving capability is to simply break the detector active area into many distinct areas or pixels, so that each can register a photon independent of the others; and when they do, only the pixel or pixels that detected a photon suffers a dead time and recovery time. Thus we have a multiple-pixel device where each pixel cannot resolve photon number, but taken together they can resolve as many photons as there are separate pixels (if those photons happen to hit different pixels). For small numbers of pixels, requiring the photons to hit different pixels can be an issue, but as the number of pixels increase, the probability of hitting the same pixel with another photon decreases, resulting in a much more faithful approximation to true photon-number-resolving capability.

Before describing specific PNR detectors we should clarify what is meant by “photon-number-resolution.” It is important to lay out the degrees of photon-number-resolution that a detector can have. First we note that as mentioned earlier, photon-number-resolving does not mean that one determines the number of photons incident on the the detector. Without 100% detection efficiency, the measured number is at best just a lower estimate, and with dark counts it is not even that. This is particularly an issue for detectors with very low efficiency. In addition we attempt to categorize the degree of PNR capability into three groups defined as (a) “no PNR capability” for devices that are typically operated as a photon or no-photon device, (b) “some PNR capability” for devices made of multiple detectors that individually have no PNR capability and thus are limited in the maximum photon number that can be resolved to the number of individual detectors, and (c) “full PNR capability” for devices whose output is inherently proportional to the number of photons, even if their detection efficiency is low and their proportional response ultimately saturates at high input photons levels. (We are assuming relatively narrow band light incident on these detectors so that a detector with an output proportional to the incident energy is used to provide information on photon number, rather than the energy of those photons.) While this categorization is somewhat arbitrary, it is of some use in understanding the types of mechanisms used to produce PNR capability.

1. Superconducting tunnel junction (STJ)-based detector

One of the first superconducting photon-number-resolving detectors was the superconducting tunnel junction detector.^{258,259,305} In it photons are absorbed in a thin superconducting layer. The absorbed energy results in many broken Cooper pairs (quasiparticles) because the photon energy is ≈ 1000 times the energy needed to break Cooper pairs. That superconducting layer is separated from a second superconducting layer by an insulator that is thin enough (≈ 1 nm) to allow significant tunneling of the quasiparticles. A small bias voltage across this “superconducting tunnel junction” results in a current flow that is proportional to the photo-generated quasiparticles. A small magnetic field parallel to the barrier, along with a bias voltage that is low enough, prevents unbroken Cooper pairs from tunneling across the junction. As the device is operated significantly (≈ 10 times) below the super-

conducting critical temperature, there are many fewer thermally generated quasiparticles than photo-generated quasiparticles, so single-photon detection is possible.

Because the current produced by this device is proportional to the incoming photon energy, it can resolve photon number. It has been demonstrated for wavelengths between 200 nm to 500 nm, limited on the long wavelength end by its energy resolution (≈ 100 nm at a wavelength of 300 nm). Devices have been demonstrated with detection efficiencies of $>45\%$ as estimated by reflectance and transmittance calculations at counts rates of ≈ 10 kHz at an operating temperature of 0.37 K.³⁰⁵ Background count rates are very low ($<0.1\%$ of photo-generated counts) and mostly limited by electronic noise, although thermal blackbody photons may also contribute.

2. Quantum-dot field-effect transistor-based detector

The QDOGFET detector, as discussed earlier, uses photo-generated charges to modulate electrical conductance and that modulation is proportional to those charges, thus this device has PNR capability and has been demonstrated with a detection efficiency of $\approx 2\%$ at 805 nm.^{265,307,308} This implementation was shown to distinguish 0, 1, 2, and greater than 3 photons, with the percent of correct assignments for these four bins being 94%, 89%, 83%, and 90%, respectively. As shown in Table II, the QDOGFET has a low detection efficiency (2%) with a repetition rate of 50 kHz and a very low dark-count probability of 0.003/gate.

The quantum dot detector based on modulation of a resonant tunneling through a barrier also has been demonstrated to have a range of few photons of PNR capability with detection efficiency of $\approx 12\%$ at 550 nm with and a dark count rate of 2000/s (Ref. 175) (Another implementation of this scheme showed linear operation which indicates the potential for PNR operation³⁰⁶). The dark count rate can be improved by an order of magnitude at a cost of reducing the detection efficiency to 5%. The operating temperature of this detector is 77 K, although faster operation was obtained at 4 K.

3. Superconducting nanowire-based single-photon detector

In Sec. III B 4, we discussed the principle behind superconducting-nanowire single-photon detectors. Two schemes have recently built upon that principle to demonstrate devices with some photon-number-resolving capability. Both achieve this by using several distinct nanowires to fill the active area rather than just a single nanowire.

The first of these schemes, the parallel-SNSPD,²⁶² uses nanowires connected electrically in parallel. The currents through the parallel wires are summed so that the single analog output signal is proportional to the number of wires that have gone normal due to incident photons. This arrangement offers the potential of even faster operation speed than the already fast single SNSPD, because the inductance of the individual wires is much lower than the longer single-wire meander of the original SNSPD, whose temporal response is

inductance limited.³²⁵ This scheme was demonstrated with niobium nitride (NbN) nanowires 100 nm wide with a capability of counting up to four photons, a dark-count rate of 0.15 Hz, and a repetition rate of 80 MHz. While the parallel-SNSPD performs well relative to other photon-number-resolving detectors in regards to dark-count rate and repetition rate, as shown in Table II, most other detectors outperform the parallel-SNSPD detection efficiency of 2% at 1300 nm.²⁶²

The second scheme also runs parallel wires, but does so as completely separate detectors with individual outputs, thus the result is a digital output i.e., the number of output pulses gives the number of photons detected. This scheme was demonstrated in a system of four separate wires with a reported system detection efficiency of 25%.³¹⁹

4. Superconducting transition edge sensor

The superconducting transition edge sensor operates as a bolometer, that is electromagnetic radiation is absorbed, and then that absorbed energy is detected as a rise in temperature. To achieve the extreme sensitivity required to detect the energy of a single photon, the heat capacity of the absorber must be made extremely small and the thermal sensor must exhibit a large response to a small temperature change. As a thermal device which measures energy absorbed, its output is proportional to the number of photons absorbed, thus it can provide photon-number resolution.

The extreme temperature sensitivity is achieved by constructing the thermal sensor from a thin layer of superconducting material (deposited on an insulating substrate) made to operate at a temperature in its transition between superconducting and normal resistance, so a slight change in temperature yields a large change in resistance. The device is maintained at this temperature through negative electro-thermal feedback. This works by applying a constant voltage bias across the film which increases the temperature of the electrons in the sensor film above the temperature of the substrate. When a photon is absorbed, the temperature of the sensor rises, which increases its resistance, which in turn reduces the current flowing through the sensor and thus reduces the Joule heating of the device. Thus the constant voltage bias and this electro-thermal feedback work to maintain the sensor at a set temperature within its superconducting transition temperature region, and the signal due to a photon is seen in a reduction in the current flowing through the sensor. Further sensitivity is achieved by measuring that current change using a superconducting quantum-interference device (SQUID) array.

The heat capacity of the sensor is reduced by fiber coupling the light to the device. By placing the fiber end just a few tens of μm from the sensor, the sensor can be made small, typically 25 μm across. In addition, operating at the low temperatures required for the superconducting transition operation further lowers the heat capacity. Note that the relevant heat capacity is that of the electrons in the superconductor and it is important that the thermal link between these electrons and the phonons in the substrate is low, which is the case at the temperatures of these devices, typically ≈ 100 mK. This weak thermal coupling of the electrons to phonons provides a link

to a thermal heat sink that allows the electrons to slowly cool after quickly heating up upon photon absorption.

Since single-photon sensitivity was first demonstrated in the visible and IR,³²⁶ TES devices of high efficiency have been demonstrated with superconductors made of tungsten,²⁹⁹ titanium,^{301,303,327} and hafnium,³⁰⁰ and because they rely on simple absorption of the incident radiation followed by conversion to heat, their wavelength sensitivity can be tailored by appropriate antireflection coatings on the sensor surface. And most recently these devices have been fabricated using a design that self-aligns the fiber to the sensor area, facilitating reliable and robust high-efficiency assembly and construction, important steps toward a scalable detector.³²⁸

From Table II, we also see that the highest detection efficiency among PNR detectors is achieved by the transition-edge sensor (TES) detectors,²⁹⁹ with a detection efficiency of 95% for an incident wavelength of 1556 nm and 81% to 98% at 850 nm.^{300–302} We also note that these detectors provide some of the best visibility between photon-number-resolved peaks of any visible detector.²⁵⁷ Despite these high detection efficiencies and very low dark-count rates, drawbacks generally include a slow response of ≈ 100 ns and low maximum counting rates of ≈ 100 kHz (although Ref. 301 reports maximum count rates up to 1 MHz), and the need to operate at temperatures less than 100 mK.²⁵⁷

5. Visible light photon counter

As seen in Table II, another detector that achieves quantum efficiencies almost as high as the TES is the visible light photon counter,^{113,264} with a detection efficiency of up to 88% at 694 nm.²⁹⁵ A photon incident onto a VLPC detector will first encounter an intrinsic silicon layer followed by a gain layer that is lightly doped with arsenic (see Fig. 9, and Fig. 1 of Ref. 264). An incident photon can be absorbed either in the intrinsic silicon layer or the doped gain layer, creating an electron-hole pair. A bias voltage of 6 V to 7.5 V accelerates the electron (hole) away from (toward) the gain region. The gain region containing the As impurities lies 54 meV below the conduction band. Holes that are accelerated in the gain region impact ionize these impurities,

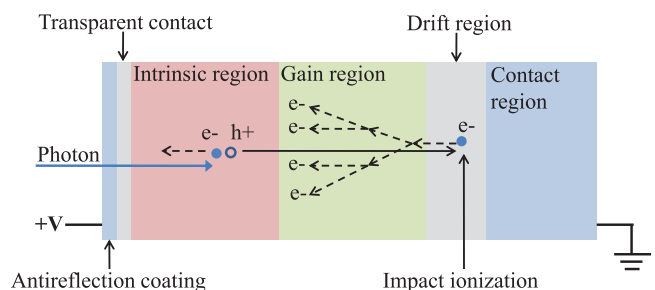


FIG. 9. (Color) Principle of operation of a visible light photon counter (VLPC). A single photon absorbed in the intrinsic region creates an electron-hole pair. The applied voltage accelerates the electron towards the transparent contact on the left, and accelerates the hole to the right. The gain region is doped with As impurities. Holes accelerated into the gain region impact-ionize these impurities, exciting donor electrons into the conduction band. These electrons are accelerated towards the transparent contact and create additional impact ionization events, resulting in avalanche multiplication (Ref. 264).

exciting donor electrons into the conduction band. These scattered electrons create further impact ionization events, resulting in avalanche multiplication. Assuming a single-photon absorption event always creates an electrical signal of the same magnitude, then the output electrical signal should simply be proportional to the number of detected photons. In practice, however, detectors that rely on multiplication gain have excess noise referred to as gain noise due to the fact that single-photon absorption does not always produce an electrical signal of the same size. If the multiplication noise is too large (as it is for SPADs, for example), then photon-number resolution is very difficult or impossible. The VLPC, however, demonstrates nearly noise-free multiplication. The first reason is that due to the partial overlap of energy states of adjacent As impurities, holes left behind in the impurity state after impact ionization travel very slowly via conduction hopping, preventing the holes from producing further impact ionization events. Single-carrier multiplication (in this case, only the electrons are multiplied) has been shown to result in lower multiplication noise.²⁶⁴ The second reason for the low multiplication noise is that low electric fields are required because the As impurities are only 54 meV below the conduction band. This results in little variation in the time between ionization events, which has also been shown to reduce multiplication noise. This low multiplication noise is what allows for demonstrated photon-number resolving capability of the VLPC of photon numbers up to six (the probability of error in making the decision increases from 0.01% for zero photons to 11.3% for six photons).

The number resolution of the VLPC is due to the fact that the charge multiplication resulting from an incident photon is localized to spot a few microns across, so only that region suffers a dead time. The rest of the detector (typically 1 mm in diameter) remains ready to register additional photons with the output signal being the sum of those output pulses. With this localized dead region being such a small fraction of the total detector area, the number-resolved operation can be nearly complete, but one must be aware of this mechanism and avoid focusing the light too tightly on the detector or number resolution will be limited.²⁶⁴

While the efficiency and photon-number-resolution of the VLPC are impressive, the repetition rate (100 kHz) is low and the dark-count rate (20 kHz) is high.²⁶⁴ Very similar in design to the VLPC is the Solid-State Photomultiplier (SSPM),²⁹⁷ which has very broad spectral sensitivity ranging from 400 nm to 28 μm . The width of this range, while quite remarkable, has the drawback that it requires additional effort to shield the detector from any of the long-wave IR photons that might be out of the wavelength band of interest. In addition the availability of these detectors is very limited.

6. Other photon-number-resolving detectors

Other approaches to PNR detectors that we do not have the space to discuss in detail include the SPAD array²⁸⁴ (simply achieving photon-number resolution by having the optical mode impinge upon an array of parallel SPADs) that are read out individually²⁸⁴ or summed to give a single output

pulse with amplitude proportional to photon number.^{279,280} the time-multiplexed SPAD (Refs. 234, 283, 329) (This uses essentially the same idea as the spatial SPAD array, but splits up the mode into many temporal modes rather than many spatial modes. A detailed performance analysis can be found in Ref. 266.), and the charge integration photon detector (CIPD) (Ref. 263) (an InGaAs PIN photodiode connected to the gate of a GaAs junction gate field-effect transistor). The performance of these approaches relative to other PNR detectors can be seen in Table II.

One recent approach uses a single SPAD as a photon-number resolving detector by measuring the slope of the avalanche rise (before saturation) to discern information about the number of incident photons.^{267,276} This is done in conjunction with a self-differencing circuit that greatly reduces the size of the capacitive transient of the APD, which allows lower overbias voltages and lower thresholds to be used. It is reported that the combination of these advantages provides photon-number resolution for up to four photons at a wavelength of 1550 nm, detection efficiency of 10%, repetition rate of 622 MHz, and a dark-count rate of less than 2×10^{-6} per gate.²⁶⁷

D. Unique approaches to single-photon detectors

Other approaches to single-photon detection that are less well-known than the approaches discussed in Secs. III A–III C include QVDs,²⁶⁸ a proposal for a high efficiency PNR detector using an atomic vapor absorber, and a proposal for a quantum nondemolition (QND) single-photon-number-resolving detector that uses giant Kerr nonlinearities.²⁷⁰

QVDs are based on heat (Q)-to-voltage (V) conversion and digital (D) readout and rely on the thermoelectric effect that occurs when a junction between dissimilar materials is heated. Although theoretical analysis claims that such detectors offer the potential to count at rates of 100 MHz, photon counting in the visible using this method has yet to be demonstrated.²⁶⁸

It has been proposed that an atomic vapor with a three-level Λ -system plus an additional level can be used as the basis of a high efficiency PNR detector.^{269,330} The scheme relies on the three-level Λ -system plus an escort pulse to allow an incoming photon to transfer one atom to a metastable level where a second laser can cycle the atom many times in a closed two-level system, with the scattered photons being the indicator that a photon has been absorbed. The reliance on an atomic vapor absorber offers the potential for high absorption efficiency, and the cycling transition allows for many scattered photons for each atom transferred, which means high detection efficiency can be achieved. And because there would be a direct correspondence between the number of incident photons absorbed and the number of atoms undergoing the closed cycling transition, this scheme would be photon-number resolving.

A quantum nondemolition (QND) measurement is one where the state is determined, but is not destroyed in the measurement so that the now-known state remains available for other uses. Such a measurement for a photon-number state was proposed by Imoto *et al.*³³¹ and discussed later in

detail by others.^{270,332,333} The principle is to co-propagate the weak signal light pulse, whose number of photons is yet to be determined, with a stronger light pulse in a highly nonlinear medium. The intensity of the signal pulse changes the refractive index of the medium, which can then be seen as a phase change in the stronger copropagating light pulse. The key difficulty is that for the unknown few-photon state to produce a resolvable phase change in the copropagating pulse, the medium must have a very large optical nonlinearity. The photonic interactions such as Kerr-nonlinearity or cross-phase modulation for most media typically do not have large enough nonlinear coefficients. While generally far from implementation because of this difficulty, possible candidate media for the QND detection can be optical fiber, a high-quality factor cavity,^{334,335} and electromagnetically induced transparency (EIT) in an atomic ensemble.^{270,333} Recently Pryde *et al.*³³⁶ reported a QND measurement on the polarization state of single photons. It was pointed out and clarified that such a measurement on the polarization state is distinct from a QND measurement of photon number.^{337,338}

E. Electronics for single-photon detectors

As we have seen, single-photon detectors use a range of physical effects to detect a photon, however there is an important trend: most detectors work close to a critical regime so that a single photon changes the regime of operation. In the case of avalanche photodiodes, the p-n junction is reverse biased with a voltage that is somewhat higher than the breakdown voltage, so any single free carrier inside that p-n junction can start an avalanche. In a superconducting nanowire detector, the wire is biased with current just below the level that would drive the wire normal. The electronics in these devices is used to set correct bias voltages or currents, to monitor sudden changes of detector properties due to photoelectronic detection, and to return the device to its normal regime. In what follows, we discuss electronics design efforts specific to avalanche photodiodes, as that has been an area of significant effort and detection improvements.

A Geiger-mode avalanche photodiode operates reverse biased at a voltage V that is above the breakdown voltage V_b . A single free carrier (generated via a photoelectronic process) injected into the depletion layer triggers a self-sustaining avalanche. The current rise time is usually less than 1 ns. This current continues to flow until the bias voltage V is dropped. This process, referred to as quenching, is a main cause of dead time, because the detector cannot respond to incoming photons until the quenching is completed and the bias voltage is restored. Once the bias voltage is restored, the device is then ready to detect another photon. The operation just described requires a special circuit that does the following:

- detects the leading edge of the current pulse that corresponds to an avalanche,
- generates an output pulse exhibiting minimal jitter with respect to the avalanche pulse,
- lowers the bias to quench the avalanche, and
- restores the photodiode voltage to the operating level $V > V_b$.

If a detector is gated, then the circuit must apply reverse bias to the detector in synchronization with the incoming optical pulses and discriminate between pulses due to bias voltage transients and actual avalanche current, in addition to the above operations.

Given the numerous tasks required of the detector electronics, the features of the circuit dramatically affect the operating conditions of the detector and, as a consequence, the detector's overall performance. The quenching mechanisms can be of three types: passive quenching, or active quenching circuits, or a combination of the two.

In passive systems, the avalanche current quenches itself. This approach is implemented with a very simple circuit – the photodiode is biased through a resistor that is small compared with the diode's resistance when no avalanche is present and large compared with the diode's residual resistance during avalanche process, typically 1 M Ω to 100 k Ω . When an avalanche occurs, the high avalanche current flowing through the bias resistor results in a voltage drop across that resistor, reducing the voltage across the diode to close enough to the diode breakdown voltage that statistical fluctuations in the current can cause the avalanche to stop. Once the avalanche current has stopped, the voltage across the diode rises again to its initial bias level and is ready for the next photon. The avalanche is detected by a standard comparator.

This arrangement was employed in the early experiments with avalanche diodes in Geiger mode.^{339,340} Pulses detected in this way have a very sharp front and an exponential tail that corresponds to reverse-bias voltage recovery. This process typically takes a few microseconds. During the recovery process, the detector regains the ability to detect single photons, but because the excess voltage has not yet reached its normal value, its detection efficiency varies in time. Also, if a second photon arrives during the recovery time, the comparator can miss it because its threshold might be higher than the recovering voltage across the p-n junction. Even if the detection electronics does detect a photon during the recovery time, the time between absorbing a photon and issuing an electronic pulse will differ from that of an isolated photodetection, increasing overall timing jitter. Under these conditions, an accurate photon count requires the use of low light levels to guarantee a small probability that a second photon is absorbed by the detector during its recovery time. Unfortunately, correcting count losses due to such recovery time by applying correction protocols originally developed for nuclear detectors leads to inaccuracies. This is because those detector systems have different dead time characteristics. Either (a) their dead time is unaffected by what happens during that dead period or (b) there is a mechanism where events occurring during the dead period, such as the receipt of an additional photon, causes that dead period to be extended.

There have been many attempts to improve single-photon detectors based on passive quenching. It has been shown that photon timing accuracy can be improved somewhat if a very low electronic level threshold is used.^{341,342} However, lowering the threshold can result in false detections, as noise can trigger the circuit. Another idea to improve detection timing jitter is by using a constant-fraction trigger circuit³⁴³ instead of a simple threshold trigger. Unfortunately, this

approach is only partially effective, because the very shape of the avalanche signal depends on the reverse-bias voltage. Therefore, during the dead-time recovery transient, when the reverse-bias voltage is rising, the rise time of the avalanche changes (the lower the bias voltage, the longer the rise time). We see that despite the apparent simplicity of the detector electronics, the practical use of passive quenching limits, sometimes significantly, detector performance. Also, attempts to improve the photon counting rate require more complex electronics, an approach that defeats the advantages of a simple circuit.

Another passively quenched SPAD scheme has recently been developed and has demonstrated some improvements. This scheme integrates the load resistor monolithically with the SPAD, which greatly reduces the device capacitance and the time for the passive quenching to occur. This in turn reduces the total flow of charge through the SPAD which results in lower afterpulse probabilities. This scheme, with the load resistor integrated with the SPAD, has been referred to as a negative-feedback avalanche diode (NFAD) to distinguish it from a SPAD with hybrid passive quench circuitry.²⁸⁹ In addition, because of the compact design, NFAD arrays can be implemented where the detectors are in parallel and the output pulse amplitude provides some photon-number resolution, as each NFAD can fire and recover independently. NFADs have been implemented with InP diodes with efficiencies of 3% to 7% at 1.5 μm and pulse durations of 30 ns to 100 ns, and maximum count rates could extend as high as 10 MHz.³⁴⁴ Similar to the NFAD array design which offers the potential of number resolution through discrete devices, a continuous version has been demonstrated in an InGaAs avalanche diode using self quenching and recovery in a localized region. Thus an absorbed photon leaves the rest of the detector area able to respond to another incoming photon, with the output being the sum of all the individual avalanches.²⁹¹

The basic idea behind active quenching is to detect the rise of an avalanche pulse and control the reverse bias voltage accordingly. That is, upon a detection of the rise of the avalanche pulse by a comparator, the bias voltage source quickly lowers the reverse bias to below the breakdown voltage V_b . After some hold-off time, defined by the lifetime of free and trapped carriers in the avalanche region, the bias voltage V is restored.

The main advantages of active quenching are the fast switching from Geiger mode to quenched mode, and the well-defined avalanche and reduced dead time. The idea is fairly simple, but there are many design issues to consider. Also, even though the timing jitter is significantly reduced, some transient effects that impact timing and detector sensitivity remain. The first actively quenched circuit was reported in 1975.³⁴⁵ A few years later, in 1981, its ability to reduce detection timing jitter was demonstrated,³⁴⁶ and the fast gating of a photodiode was attempted.³⁴⁷

Modern actively quenched detectors can have electronic photodetection jitter below 100 ps and dead times below 50 ns. The dead time is currently limited by carrier trapping time inside the avalanche zone of the photodiode, and not by the quenching electronics. However, transient effects can still complicate the behavior of detectors immediately before

and immediately after the quenching pulse, contributing to so-called twilight effects.^{80,348}

For detectors with high dark-count rates, gated operation is necessary. There are two types of gated circuits. The simplest has a fixed time for the APD bias to be applied. In this case if an avalanche occurs, it is quenched at the predetermined end of the gate time. The alternative uses an active circuit that terminates the bias as soon as an avalanche is detected after the gate is turned on. This has the advantage of reducing the total charge flow through the APD, which reduces the number of trapped carriers and, as a result, the rate of afterpulsing.^{349,350} This scheme has become more practical as integrated quenching electronics has been developed.³⁵¹

Both gating schemes rely on switching the bias voltage from $V > V_b$ to $V < V_b$ and back. These rapid voltage changes cause the diode to act like a damped capacitor when no avalanche occurs. Because of these large background pulses, it can be hard to pick out the avalanche signal unless efforts are made to cancel the transient voltages, or gate times are made long enough that the transients can be temporally discriminated by the electronics.

There are several strategies to deal with these transients. An intuitive approach is to send the gate pulse to both the photodiode and a capacitor-resistor pair that mimics the transient in a p-n junction with no avalanches. The same result can be achieved using distributed impedances that create two identical, but temporally displaced, output pulses.³⁵² Then one pulse is simply subtracted from the other, before being sent to a comparator. If no avalanche is present, the transient effects cancel. If an avalanche is present, it will be easily revealed. However, such matching requires careful study of the photodiode's properties under the operating conditions (bias voltage, temperature, etc.) and adjustment if either the photodiode or its operating conditions change.

There are other schemes for canceling these transients. It has been proposed that two, rather than one avalanche photodiodes are used with their outputs arranged to cancel transients from one another.³⁵³ However, the two detectors must be nearly identical. One can overcome this requirement by using two subsequent pulses from the same APD, with one pulse delayed in time to overlap the other.²⁴⁹ In this case, no prior information about the photodiode is needed, but there is a problem if adjacent pulses each have an incident photon. Only the first one will be detected by the electronics, as the second one will be canceled by the first, resulting in undercounting. Also, if the gating must be synchronized to a clock, random gating (necessary for cw heralded-photon detection) cannot be used.

There is another proposal where the output of the detector is passed through an integrator. In that case, the passive response of the photodiode is removed by integration, while the avalanche will appear as an offset due to an extra avalanche peak. The problem here is that an avalanche is detected only after the gate ends, which erases information as to when within the gate pulse the avalanche occurred.³⁵⁴

Another related approach to dealing with transients works in a somewhat inverse fashion. In this scheme a discriminator threshold is set to sense the negative going transient at the end of the gate pulse. This transient is due to the

capacitance of the detector discharging. When an photon triggers an avalanche, that avalanche discharges the detector capacitance so the negative-going pulse is reduced, and is not seen by the comparator. Thus the absence of the comparator firing indicates the detection of a photon.^{288,355} This has the advantage of suppressing afterpulsing by allowing for shorter gate duration and thus fewer filled trap sites.

Finally, there is a scheme aimed at reducing afterpulsing in InGaAs SPADs by reducing current flow in an unusual manner.³⁵⁶ The scheme uses the fact that while an incoming IR photon triggers an avalanche, that avalanche itself results in the emission of other photons that may be visible. A Si SPAD registers these secondary photons, so effectively the system works by up conversion from the IR to the visible. The advantage in afterpulsing is gained because the IR SPAD does not need any processing electronics for its avalanche, greatly reducing its total capacitance. This greatly reduces the charge through the diode, resulting in fewer filled traps that must be emptied. While just a proposal, calculations suggest high detection efficiency and low afterpulse probabilities are possible.

A detailed review on the history of detector electronics can be found in Refs. 349, 357. Modern trends in developing electronics for SPADs that require gating are found in Ref. 100.

IV. APPLICATION CASE STUDY: QUANTUM COMMUNICATION

Single-photon sources and detectors are key to photon-based quantum communication. We use this area as a case study of how the real characteristics of sources and detectors impact performance in practice. In particular, we look at QKD and quantum repeaters and how the nonideal natures of single-photon sources and detectors directly affect the communication rates, the link lengths, and the security. To illustrate the effect that source and detector properties may have on QKD protocols, we consider the example of the Bennett and Brassard QKD protocol of 1984 (BB84) protocol which uses polarization encoding.¹⁷ While decoy-state methods using faint laser pulses^{358,359} may reduce the need for single-photon *source* development for QKD, the characteristics of single-photon *detectors* will still greatly influence the practically achievable performance of QKD protocols in general, and we note that specific security attack schemes have focused on particular detector characteristics.^{360–363} Additionally, the development of quantum repeaters, a key enabling technology for long-distance quantum communication, will depend critically on the performance of both single-photon sources and single-photon detectors.^{32,364}

We first consider BB84,¹⁷ a QKD protocol, whereby a common set of random bits are generated at two ends of a communication link for later use as a secret key in sending encrypted messages. It is important to note that although we assume that the photon polarization is used to encode the qubit in this example, polarization is just one of many possible ways to encode qubits in photons. For example, time-bin qubits are preferred at telecom wavelengths.³⁶⁵

In the BB84 polarization-encoded scheme, the sender (Alice) encodes random zeros or ones in the polarization state of a single photon. The encoding is done by randomly setting the photon's polarization to either horizontal, $|H\rangle$ or vertical, $|V\rangle$ to represent 0 or 1 or by setting the polarization to diagonal, $|D\rangle$ or anti-diagonal $|A\rangle$ to represent 0 or 1. The receiver (Bob) randomly selects either the HV or DA bases to analyze the polarization of the photons he receives. By an open authenticated communication channel, Alice and Bob reconcile the preparation and measurement of each bit so that they know which photons made it through the optical link and were detected by Bob, and which of these were analyzed in the basis that matched the sending basis. They discard any bit that either was not received by Bob or was analyzed in the wrong basis, leaving what is referred to as “sifted key.” This open reconciliation channel contains only the basis and which photons were received, not the measurement result, so an eavesdropper (Eve) of this open channel would not learn if the bit was a 0 or 1. Only by intercepting and receiving the photon pulse would Eve have a chance to learn the value of the bit sent, but because only a single photon was sent, after making her measurement Eve would have to prepare a new photon to send to Bob. But because Eve would not know if the sending basis was HV or DA she would send the photon in the wrong basis 50% of the time. That would mean that some of the time that Alice sent a 0 in a particular basis, Bob would receive a 1 in that same basis and vice versa. This telltale error can be detected by Alice and Bob by comparing a subset of their common bits, and additional measures would have to be taken to maintain security.¹⁵ Those additional measures consume some of the sifted key bits, but create a shorter “secret key” that greatly reduces the amount of knowledge that Eve can have of the resulting secret key shared by Alice and Bob.

While acknowledging that the subsequently developed decoy-state scheme has provided a way to address this issue, the QKD just described assumes the bit to be transmitted is a single photon, for if the photon pulse encoding the bit contained more than one photon then Eve could potentially detect just one photon while letting the other(s) continue unperturbed to Bob, who would not detect Eve's presence because no error was created.

While faint laser pulse sources were the easiest and first sources used for QKD implementations, two single-emitter systems, namely quantum dots and nitrogen-vacancy centers, have been used as single-photon sources in proof-of-principle QKD experiments.^{103,138,366} In principle, for a given secure communication rate, single-emitter-based QKD systems can achieve longer key transmission distances than faint laser pulse systems. This is because the nonzero two-photon emission probability decreases the performance of faint-laser systems relative to the performance of single-emitter systems due to the increasing loss with increasing distance. With faint-laser systems that have loss between the source and detector, there is always some probability that the *detection* of a single photon corresponds to the *emission* of two or more photons, with the other photon(s) being lost in transmission. This issue is avoided by operating the source such that the probability of single-photon emission, p , is much less than one, so that the probability of emitting two or more photons,

$\sim p^2$, is negligible. Operating at lower mean photon number means that Bob will record zero-photon time bins more often, thus decreasing the bit rate. In addition, since Bob must look at more time bins to obtain the same number of useful events, the contribution of noise (dark counts and stray photons) in Bob's detectors increases. This is an example of a nonideal characteristic of a photon-counting detector that will result in a greater bit-error-rate, yielding a shorter secret key for a given length of sifted key. In contrast, the emission rate of single-emitter sources does not need to be operated with $p \ll 1$, since by definition there is zero probability of a two-photon emission (or zero to a significant degree in implemented systems). The result is that the secure communication rate of single-emitter QKD systems, relative to faint-laser pulse systems, increases with increasing loss.³⁶⁶ Another way of saying this is that since loss increases with distance, single-emitter-based QKD systems can achieve longer transmission distances than faint laser pulse systems for a given secure communication rate. To date, however, technical challenges have limited single-emitter QKD demonstrations to relatively modest distances.^{103,138,366}

In addition to source issues, the nonideal nature of the photon-counting detectors used in a QKD system also affects its performance. As we have already discussed how detector dark counts impact a QKD system, we move on to discuss the effect of detector efficiency, which has the same impact as link loss. It means that for a given rate of photons incident on the detector, Bob will detect zero photons more often, thus decreasing the bit rate. This will also increase the contribution of noise in Bob's detectors, resulting in a greater bit-error-rate and yielding a shorter secret key for a given length of sifted key. The result is that the secure communication rate of a detector increases with increasing efficiency.

Other detector properties, such as detector dead time, also affect the performance of QKD protocols. If the dead time of a detector is greater than the smallest possible time-bin spacing allowed by the single-photon source, then increased dead time results in a decreased communication rate. It has also been shown that detector dead time can lead to the leaking of information or even be directly manipulated by third party to gain information from the quantum channel.^{360,362,363} In addition to these properties it has been shown that even small differences in detector timing jitter can leak secret key information from these protocols.³⁶¹

To enable quantum communication for networks over long distances, quantum repeaters will be essential. Quantum repeaters work by breaking the total communication distance into a series of shorter links, with quantum memories being required to create entanglement between the end nodes of each link. At least one quantum repeater protocol has been developed that relies only on *single*-photon sources (as compared to a source of correlated *pairs* of excitations) and single-photon detectors, and whose fundamental fidelity would be theoretically equal to one for perfect sources, detectors, and other components.^{32,364} As with QKD protocols, the performance of quantum-repeater protocols depends on the characteristics of the sources and detectors used in practice.^{32,364} For example, for the quantum-repeater protocol described in Ref. 364, detector dark counts and multiple-photon emission

can correspond to states other than the desired entangled state, decreasing the fidelity. As an example, for the parameters listed in Ref. 364 (communication length of 1000 km, characteristic absorption length in the fiber of 22 km corresponding to the telecommunications wavelength of 1.5 μm , memory efficiency of 0.9, detector efficiency of 0.9, and single-photon emission success probability of 0.95), the detector dark-count probability of each detector must be smaller than 4.6×10^{-6} and the two-photon emission probability for each source must be smaller than 3.7×10^{-4} for a final fidelity of 0.9.

In summary, the non-ideal nature of both single-photon sources and single-photon detectors can greatly affect quantum communication protocols. The sources, by not being truly on-demand, reduce throughput, limit link length, and can compromise security. And by not being reproducible and indistinguishable single-photon states, quantum communication systems will suffer reduced overall efficiency that will ultimately make a scalable system unachievable. As with non-ideal sources, photon-counting detectors with nonideal characteristics like finite detection efficiency, non-number resolving, non-zero timing jitter, finite dead time, etc., have similar impacts on practical quantum communication systems. In addition, because detectors convert the quantum state to classical information they are also subject to direct attacks on security that cannot rely on fundamental principles like quantum mechanics to be detected.

V. SUMMARY

As should be clear by now, the field of single-photon sources and detectors is of great interest and importance to many applications, and the importance of these applications is driving many current efforts to improve these devices. The field has now reached a certain level of maturity, with devices finding their way into many off-the-shelf components. Today it is possible to find nearly ideal devices when only one parameter is important, but performance of other parameters is often compromised. Examples of such trade-offs for sources is low $g^{(2)}(0)$ versus the deterministic character of photon emission; and for detectors an example is the efficiency versus speed trade-off seen in the TES detector. Much of the current work in this field involves studying and addressing such trade-offs.

Specifically for sources, while initial efforts were focused mostly on increasing brightness and generation efficiency, current improvement efforts are more driven by the requirements for particular applications and often deal directly with improving more than one characteristic simultaneously, as it is now well understood that heroic results in improving a single parameter are often of little practical use. These present multi-parameter efforts include better single-photon state accuracy [in the form of lower $g^{(2)}(0)$], and higher degrees of indistinguishability of single-photon output states which is particularly important for many quantum-information applications. These improvements involve engineering of photon-state parameters such as designing sources to produce uncorrelated joint spectral distributions (i.e., factorable states). Another example of state engineering is the multiplexed PDC source which is an attempt to increase

single-photon emission efficiency and reduce multi-photon emission [or equivalently, reduce $g^{(2)}(0)$], simultaneously. There are also significant efforts toward scalable devices with more compact and robust designs, which are also critical to the ultimate development of any large scale photonic systems that might be required for information processing, metrologic sources, or even complicated quantum-measurement arrangements. This focus on scalability is one of the drivers that has moved source efforts from bulk PDC to fiber FWM, now to isolated quantum systems (particularly at room temperature) and silicon photonic waveguides.

For detectors, while it is clear that SPADs are the workhorse devices for a great many applications, there are needs for detectors that exceed what is available with SPADs for individual properties. As a result, there is much work to improve detectors, with improvement directions including higher efficiencies, with some already approaching 100%, lower timing jitter, with sub-50 ps demonstrated, reduced afterpulsing, and better photon-number resolution. As with sources, there are also efforts toward improving more than one detector parameter simultaneously such as giving the high-speed SNSPD detectors some photon-number resolution by implementing multiple element detectors or switched multiplexed detectors that reduce dead time and afterpulsing effects simultaneously, or IR upconversion schemes that have high efficiency, high count rates, and low background rates. One can certainly expect these trends toward improving multiple parameters for both sources and detectors to continue for the foreseeable future, as there is plenty of room for improvement and there are many applications that can benefit from such improvements.

All this effort on single-photon devices requires supporting efforts in single-photon metrology, with an ultimate goal of connecting photon-counting radiometry to conventional detector and source standards that typically deal with too many photons to even consider counting.^{80,367} While this is certainly an ambitious goal, it offers a potential path toward improving radiometric measurements by many orders of magnitude, and provides a solid infrastructure for characterizing and developing better sources and detectors.

ACKNOWLEDGMENTS

We acknowledge the help and useful discussions of J. C. Bienfang, J. Chen, W. H. Farr, E. A. Goldschmidt, W. Grice, D. Herr, P. G. Kwiat, Z. H. Levine, R. P. Mirin, S. W. Nam, A. Restelli, M. J. Stevens, F. N. C. Wong, and T. Zhong. We acknowledge the partial support of the National Science Foundation (NSF) through the Physics Frontier Center at the Joint Quantum Institute.

¹C. Cohen-Tannoudji, J. Dupont-Roc, and G. Grynberg, *Photons and Atoms: Introduction to Quantum Electrodynamics* (Wiley-Interscience, New York, 1997).

²R. Loudon, *The Quantum Theory of Light* (Oxford University Press, New York, 2000).

³M. Planck, *Verh. Dtsch. Phys. Ges.* **2**, 202 (1900).

⁴M. Planck, *Verh. Dtsch. Phys. Ges.* **2**, 237 (1900).

⁵D. ter Haar, *The Old Quantum Theory* (Pergamon, Oxford, 1967).

⁶A. Einstein, *Ann. Phys.* **17**, 132 (1905).

⁷A. B. Arons and M. B. Peppard, *Am. J. Phys.* **33**, 367 (1965).

⁸A. H. Compton, *Phys. Rev.* **21**, 483 (1923).

⁹G. Lewis, *Nature (London)* **118**, 874 (1926).

¹⁰P. A.M. Dirac, *Proc. R. Soc. London* **114**, 243 (1927).

¹¹E. Fermi, *Rev. Mod. Phys.* **4**, 87 (1932).

¹²M. O. Scully and M. S. Zubairy, *Quantum Optics* (Cambridge University Press, Cambridge, 1997).

¹³R. Glauber, *Rev. Mod. Phys.* **78**, 1267 (2006).

¹⁴Technical Report on Quantum Cryptography Technology Experts Panel, Advanced Research and Development Activity (ARDA), 2004, see <http://qist.lanl.gov>.

¹⁵A. Ekert, N. Gisin, B. Huttner, H. Inamori, and H. Weinfurter, in *The Physics of Quantum Information*, edited by D. Bouwmeester, A. Ekert, and A. Zeilinger (Springer, Berlin, 2000).

¹⁶P. Shor, *Proceedings of 35th Annual Symposium on Foundations of Computer Science* (IEEE Computer Society Press, Los Alamitos, CA, 1994), pp. 124–134.

¹⁷C. Bennett and G. Brassard, in *Proceedings of IEEE International Conference on Computers, Systems, and Signal Processing, Bangalore, India* (IEEE, New York, 1984), pp. 175–179.

¹⁸A. K. Ekert, *Phys. Rev. Lett.* **67**, 661 (1991).

¹⁹C. H. Bennett, *Phys. Rev. Lett.* **68**, 3121 (1992).

²⁰H. Inamori, N. Lütkenhaus, and D. Mayers, *Eur. Phys. J. D* **41**, 599 (2007).

²¹D. Gottesman, H.-K. Lo, N. Lütkenhaus, and J. Preskill, *Quantum Inf. Comput.* **4**, 325 (2004).

²²W.-Y. Hwang, *Phys. Rev. Lett.* **91**, 057901 (2003).

²³X.-B. Wang, *Phys. Rev. Lett.* **94**, 230503 (2005).

²⁴X. Ma, B. Qi, Y. Zhao, and H. Lo, *Phys. Rev. A* **72**, 012326 (2005).

²⁵C. Bennett, G. Brassard, and J. Robert, *SIAM J. Comput.* **17**, 210 (1988).

²⁶C. H. Bennett, G. Brassard, C. Crépeau, and U. M. Maurer, *IEEE Trans. Inf. Theory* **41**, 1915 (1995).

²⁷D. Deutsch, A. Ekert, R. Jozsa, C. Macchiavello, S. Popescu, and A. Sanpera, *Phys. Rev. Lett.* **77**, 2818 (1996).

²⁸N. Gisin, G. Ribordy, W. Tittel, and H. Zbinden, *Rev. Mod. Phys.* **74**, 145 (2002).

²⁹H. J. Briegel, W. Dur, S. J. van Enk, J. I. Cirac, and P. Zoller, in *The Physics of Quantum Information*, edited by D. Bouwmeester, A. Ekert, and A. Zeilinger (Springer, Berlin, 2000).

³⁰L. Duan, M. Lukin, J. Cirac, and P. Zoller, *Nature (London)* **414**, 413 (2001).

³¹C. Simon, H. de Riedmatten, M. Afzelius, N. Sangouard, H. Zbinden, and N. Gisin, *Phys. Rev. Lett.* **98**, 190503 (2007).

³²N. Sangouard, C. Simon, H. de Riedmatten, and N. Gisin, *Rev. Mod. Phys.* **83**, 33 (2011).

³³N. Sangouard, C. Simon, B. Zhao, Y.-A. Chen, H. de Riedmatten, J.-W. Pan, and N. Gisin, *Phys. Rev. A* **77**, 062301 (2008).

³⁴C. H. Bennett, G. Brassard, C. Crépeau, R. Jozsa, A. Peres, and W. K. Wothers, *Phys. Rev. Lett.* **70**, 1895 (1993).

³⁵J. Rarity, P. Owens, and P. Tapster, *J. Mod. Opt.* **41**, 2435 (1994).

³⁶A. Stefanov, N. Gisin, O. Guinnard, L. Guinnard, and H. Zbinden, *J. Mod. Opt.* **47**, 595 (2000).

³⁷A. Migdall and J. Dowling, *J. Mod. Opt.* **51**, 1265 (2004).

³⁸T. Isohima, Y. Isojima, K. Kikuchi, K. Nagai, and H. Nakagawa, *Rev. Sci. Instrum.* **66**, 2922 (1995).

³⁹U. Lieberwirth, J. Arden-Jacob, K. H. Drexhage, D. P. Herten, R. Muller, M. Neumann, A. Schulz, S. Siebert, G. Sagner, S. Klingel, M. Sauer, and J. Wolfrum, *Anal. Chem.* **70**, 4771 (1998).

⁴⁰J.-P. Knemeyer, N. Marme, and M. Sauer, *Anal. Chem.* **72**, 3717 (2000).

⁴¹D. N. Gavrilov, B. Gorbovitski, M. Gouzman, G. Gudkov, A. Stepoukhovitch, V. Ruskovoloshin, A. Tsuprik, G. Tyshko, O. Bilenko, O. Kosobokova, S. Luryi, and V. Gorfinkel, *Electrophoresis* **24**, 1184 (2003).

⁴²I. Rech, A. Restelli, S. Cova, M. Ghioni, M. Chiari, and M. Cretich, *Sens. Actuators B* **100**, 158 (2004).

⁴³J.-P. Knemeyer, N. Marme, and M. Sauer, *Science* **283**, 1676 (1999).

⁴⁴A. Berglund, A. Doherty, and H. Mabuchi, *Phys. Rev. Lett.* **89**, 068101 (2002).

⁴⁵K. Suhling, P. French, and D. Phillips, *Photochem. Photobiol. Sci.* **4**, 13 (2005).

⁴⁶T. McIlrath, R. Hudson, A. Aikin, and T. Wilkerson, *Appl. Opt.* **18**, 316 (1979).

⁴⁷M. Viterbini, A. Adriani, and G. Didonfrancesco, *Rev. Sci. Instrum.* **58**, 1833 (1987).

- ⁴⁸S. Pellegrini, G. Buller, J. Smith, A. Wallace, and S. Cova, *Meas. Sci. Technol.* **11**, 712 (2000).
- ⁴⁹S. Personick, *Bell Syst. Tech. J.* **56**, 355 (1977).
- ⁵⁰B. Levine, C. Bethea, and J. Campbell, *Appl. Phys. Lett.* **46**, 333 (1985).
- ⁵¹G. Ripamonti, M. Ghioni, and S. Vanoli, *Electron. Lett.* **26**, 1569 (1990).
- ⁵²A. Lacaïta, P. Francese, S. Cova, and G. Ripamonti, *Opt. Lett.* **18**, 1110 (1993).
- ⁵³F. Scholder, J. Gautier, M. Wegmuller, and N. Gisin, *Opt. Commun.* **213**, 57 (2002).
- ⁵⁴A. Wegmuller, F. Scholder, and N. Gisin, *J. Lightwave Technol.* **22**, 390 (2004).
- ⁵⁵M. Legre, R. Thew, H. Zbinden, and N. Gisin, *Opt. Express* **15**, 8237 (2007).
- ⁵⁶J. Kash, J. Tsang, D. Knebel, and D. Vallett, in *ISTFA '98: Proceedings Of The 24TH International Symposium For Testing And Failure Analysis* (American Technical Publishers, 1998), pp. 483–488.
- ⁵⁷J. Tsang, J. Kash, and D. Vallett, *IBM J. Res. Dev.* **44**, 583 (2000).
- ⁵⁸F. Stellari, F. Zappa, S. Cova, C. Porta, and J. Tsang, *IEEE Trans. Electron Devices* **48**, 2830 (2001).
- ⁵⁹N. Goldblatt, M. Leibowitz, and W. Lo, *Microelectron. Reliab.* **41**, 1507 (2001).
- ⁶⁰F. Stellari, A. Tosi, F. Zappa, and S. Cova, *IEEE Trans. Instrum. Meas.* **53**, 163 (2004).
- ⁶¹S. Polonsky and K. Jenkins, *IEEE Electron Device Lett.* **25**, 208 (2004).
- ⁶²S. Soper, Q. Mattingly, and P. Vegunta, *Anal. Chem.* **65**, 740 (1993).
- ⁶³L.-Q. Li and L. Davis, *Rev. Sci. Instr.* **64**, 1524 (1993).
- ⁶⁴I. Rech, G. Luo, M. Ghioni, H. Yang, X. S. Xie, and S. Cova, *IEEE J. Sel. Top. Quant. Electron.* **10**, 788 (2004).
- ⁶⁵M. Wahl, F. Koberling, M. Pating, H. Rahn, and R. Erdmann, *Curr. Pharm. Biotechnol.* **5**, 299 (2004).
- ⁶⁶M. Gosch, A. Serov, T. Anhut, T. Lasser, A. Rochas, P. Besse, R. Popovic, H. Blom, and R. Rigler, *J. Biomed. Opt.* **9**, 913 (2004).
- ⁶⁷X. Michalet, O. H.W. Siegmund, J. V. Vallerger, P. Jelinsky, J. E. Millaud, and S. Weiss, *J. Mod. Opt.* **54**, 239 (2007).
- ⁶⁸X. Michalet, R. A. Colyer, J. Antelman, O. H.W. Siegmund, A. Tremsin, J. V. Vallerger, and S. Weiss, *Curr. Pharm. Biotechnol.* **10**, 543 (2009).
- ⁶⁹S. Felekyan, R. Kühnemuth, V. Kudryavtsev, C. Sandhagen, W. Becker, and C. A. M. Seidel, *Rev. Sci. Instr.* **76**, 083104 (2005).
- ⁷⁰A. Pifferi, A. Torricelli, L. Spinelli, D. Contini, R. Cubeddu, F. Martelli, G. Zaccanti, A. Tosi, A. D. Mora, F. Zappa, and S. Cova, *Phys. Rev. Lett.* **100**, 138101 (2008).
- ⁷¹V. C. Spanoudaki, A. B. Mann, A. N. Otte, I. Konorov, I. Torres-Espallardo, S. Paul, and S. I. Ziegler, *J. Inst.* **2**, 12002 (2007).
- ⁷²D. Klyshko, *Kvantovaya Elektronika* **4**, 1056 (1977) [*Sov. J. Quantum Elect.* **7**, 591 (1977)].
- ⁷³A. Malygin, A. Penin, and A. Sergienko, *JETP Lett.* **33**, 477 (1981) [http://www.jetpletters.ac.ru/ps/1510/article_23064.pdf].
- ⁷⁴A. Migdall, R. Datla, A. Sergienko, J. Orszak, and Y. Shih, *Appl. Opt.* **37**, 3455 (1998).
- ⁷⁵A. Migdall, E. Dauler, A. Muller, and A. Sergienko, *Anal. Chim. Acta* **380**, 311 (1999).
- ⁷⁶M. Ware and A. Migdall, *J. Mod. Opt.* **51**, 1549 (2004).
- ⁷⁷G. Brida, M. Genovese, M. Gramegna, M. Rastello, M. Chekhova, and L. Krivitsky, *J. Opt. Soc. Am. B* **22**, 488 (2005).
- ⁷⁸S. Castelletto, I. P. Degiovanni, V. Schettini, and A. Migdall, *Metrologia* **43**, S56 (2006).
- ⁷⁹G. Brida, M. Genovese, and M. Gramegna, *Laser Phys. Lett.* **3**, 115 (2006).
- ⁸⁰S. V. Polyakov and A. L. Migdall, *Opt. Express* **15**, 1390 (2007).
- ⁸¹S. A. Castelletto and R. E. Scholten, *Eur. Phys. J.: Appl. Phys.* **41**, 181 (2008).
- ⁸²G. Hungerford and D. Birch, *Meas. Sci. Technol.* **7**, 121 (1996).
- ⁸³P. Yao, V. S.C. MangaRao, and S. Hughes, *Laser Photonics Rev.* **4**, 499 (2010).
- ⁸⁴K. Greulich and E. Thiel, *Single Mol.* **2**, 5 (2001).
- ⁸⁵A. Kuhn and D. Ljunggren, *Contemp. Phys.* **51**, 289 (2010).
- ⁸⁶B. Lounis and M. Orrit, *Rep. Prog. Phys.* **68**, 1129 (2005).
- ⁸⁷M. Oxborrow and A. Sinclair, *Contemp. Phys.* **46**, 173 (2005).
- ⁸⁸D. Renker and E. Lorenz, *J. Instrum.* **4**, P04004 (2009).
- ⁸⁹H. Hertz, *Ann. Phys. Chem.* **31**, 983 (1887).
- ⁹⁰J. Elster and H. Geitel, *Ann. Phys.* **284**, 625 (1893).
- ⁹¹H. Iams and B. Salzberg, *Proc. IRE* **23**, 55 (1935).
- ⁹²V. Zworykin, G. Morton, and L. Malter, *Proc. IRE* **24**, 351 (1935).
- ⁹³L. A. Kubetsky, *Proc. Inst. Radio Eng.* **254**, 421 (1937).
- ⁹⁴K. O. Kiepenheuer, *Z. Phys.* **107**, 145 (1937).
- ⁹⁵Z. Bay, *Nature (London)* **141**, 1011 (1938).
- ⁹⁶J. S. Allen, *Phys. Rev.* **55**, 966–971 (1939).
- ⁹⁷R. McIntyre, *J. Appl. Phys.* **32**, 983 (1961).
- ⁹⁸D. E. Groom, *Nucl. Instrum. Methods Phys. Res.* **219**, 141 (1984).
- ⁹⁹S. Pellegrini, R. E. Warburton, L. J. J. Tan, J. S. Ng, A. B. Krysa, K. Groom, J. P.R. David, S. Cova, M. J. Robertson, and G. S. Buller, *IEEE J. Quant. Electron.* **42**, 071116 (2006).
- ¹⁰⁰A. Tosi, A. D. Mora, F. Zappa, and S. Cova, *J. Mod. Opt.* **56**, 299 (2009).
- ¹⁰¹X. Jiang, M. A. Itzler, R. Ben-Michael, and K. Slomkowski, *IEEE J. Sel. Top. Quantum Electron.* **13**, 895 (2007).
- ¹⁰²R. Warburton, M. Itzler, and G. Buller, *Electron. Lett.* **45**, 996 (2009).
- ¹⁰³R. Alleaume, F. Treussart, G. Messin, Y. Dumeige, J.-F. Roch, A. Beveratos, R. Brouri-Tualle, J.-P. Poizat, and P. Grangier, *New J. Phys.* **6**, 92 (2004).
- ¹⁰⁴T. Gaebel, I. Popa, A. Gruber, M. Domhan, F. Jelezko, and J. Wrachtrup, *New J. Phys.* **6**, 98 (2004).
- ¹⁰⁵E. Wu, J. R. Rabeau, G. Roger, F. Treussart, H. Zeng, P. Grangier, S. Praver and J.-F. Roch, *New J. Phys.* **9**, 434 (2007).
- ¹⁰⁶S. Kako, C. Santori, K. Hoshino, S. Gotinger, Y. Yamamoto, and Y. Arakawa, *Nature Mater.* **5**, 887 (2006).
- ¹⁰⁷A. J. Shields, *Nature Photon.* **1**, 215 (2007).
- ¹⁰⁸S. Strauf, N. G. Stoltz, M. T. Rakher, L. A. Coldren, P. M. Petroff, and D. Bouwmeester, *Nature Photon.* **1**, 704 (2007).
- ¹⁰⁹M. Hennrich, T. Legero, A. Kuhn, and G. Rempe, *New J. Phys.* **6**, 86 (2004).
- ¹¹⁰C. Maurer, C. Becher, C. Russo, J. Eschner, and R. Blatt, *New J. Phys.* **6**, 94 (2004).
- ¹¹¹M. Steiner, A. Hartschuh, R. Korlacki, and A. J. Meixner, *Appl. Phys. Lett.* **90**, 183122 (2007).
- ¹¹²S. Chen, Y.-A. Chen, T. Strassel, Z.-S. Yuan, B. Zhao, J. Schmiedmayer, and J.-W. Pan, *Phys. Rev. Lett.* **97**, 173004 (2006).
- ¹¹³E. Waks, E. Diamanti, and Y. Yamamoto, *New J. Phys.* **8**, 4 (2006).
- ¹¹⁴A. Soujaeff, T. Nishioka, T. Hasegawa, S. Takeuchi, T. Tsurumaru, K. Sasaki, and M. Matsui, *Opt. Express* **15**, 726 (2007).
- ¹¹⁵A. B. U'Ren, C. Silberhorn, K. Banaszek, and I. A. Walmsley, *Phys. Rev. Lett.* **93**, 093601 (2004).
- ¹¹⁶J. Fan and A. Migdall, *Opt. Express* **15**, 2915 (2007).
- ¹¹⁷E. A. Goldschmidt, M. D. Eisaman, J. Fan, S. V. Polyakov, and A. Migdall, *Phys. Rev. A* **78**, 013844 (2008).
- ¹¹⁸A. Hartschuh, H. N. Pedrosa, J. Peterson, L. Huang, P. Anger, H. Qian, A. J. Meixner, M. Steiner, L. Novotny, and T. D. Krauss, *Chem. Phys. Chem.* **6**, 1 (2005).
- ¹¹⁹A. Hogebe, C. Galland, M. Winger, and A. Imamoglu, *Phys. Rev. Lett.* **100**, 217401 (2008).
- ¹²⁰T. B. Pittman, J. D. Franson, and B. C. Jacobs, *New J. Phys.* **9**, 195 (2007).
- ¹²¹B. C. Jacobs, T. B. Pittman, and J. D. Franson, *Phys. Rev. A* **74**, 010303(R) (2006).
- ¹²²A. Aspect, P. Grangier, and G. Roger, *Phys. Rev. Lett.* **47**, 460 (1981).
- ¹²³P. G. Kwiat and R. Y. Chiao, *Phys. Rev. Lett.* **66**, 588 (1991).
- ¹²⁴S. Fasel, O. Alibart, S. Tanzilli, P. Baldi, A. Beveratos, N. Gisin, and H. Zbinden, *New J. Phys.* **6**, 163 (2004).
- ¹²⁵Q. Wang, W. Chen, G. Xavier, M. Swillo, T. Zhang, S. Sauge, M. Tengner, Z.-F. Han, G.-C. Guo, and A. Karlsson, *Phys. Rev. Lett.* **100**, 090501 (2008).
- ¹²⁶A. Fedrizzi, T. Herbst, A. Poppe, T. Jennewein, and A. Zeilinger, *Opt. Express* **15**, 15377 (2007).
- ¹²⁷T. Zhong, X. Hu, F. N.C. Wong, K. K. Berggren, T. D. Roberts, and P. Battle, *Opt. Lett.* **35**, 1392 (2010).
- ¹²⁸S. Takeuchi, R. Okamoto, and K. Sasaki, *Appl. Opt.* **43**, 5708 (2004).
- ¹²⁹G. Brida, I. P. Degiovanni, M. Genovese, A. Migdall, F. Piacentini, S. V. Polyakov, and I. R. Berchera, *Opt. Express* **19**, 1484 (2011).
- ¹³⁰X.-S. Ma, S. Zotter, J. Kofler, T. Jennewein, and A. Zeilinger (2010), see http://arxiv.org/PS_cache/arxiv/pdf/1007/1007.4798v1.pdf.
- ¹³¹S. D. Dyer, M. J. Stevens, B. Baek, and S. W. Nam, *Opt. Express* **16**, 9966 (2008).
- ¹³²B. J. Smith, P. Mahou, O. Cohen, J. S. Lundeen, and I. A. Walmsley, *Opt. Express* **17**, 23589 (2009).
- ¹³³A. Ling, J. Chen, J. Fan, and A. Migdall, *Opt. Express* **17**, 21302 (2009).
- ¹³⁴H. Takesue, Y. Tokura, H. Fukuda, T. Tsuchizawa, T. Watanabe, K. Yamada, and S.-i. Itabashi, *Appl. Phys. Lett.* **91**, 201108 (2007).
- ¹³⁵S. G. Lukishova, A. W. Schmid, A. J. McNamara, R. W. Boyd, and J. Carlos R. Stroud, *IEEE J. Sel. Top. Quantum Electron.* **9**, 1512 (2003).

- ¹³⁶R. Alleaume, F. Treussart, J.-M. Courty, and J.-F. Roch, *New J. Phys.* **6**, 85 (2004).
- ¹³⁷S. G. Lukishova, A. W. Schmidz, C. M. Supranowitzky, N. Lippa, A. J. Mcnamara, R. W. Boyd, and J. C. R. Stroud, *J. Mod. Opt.* **51**, 1535 (2004).
- ¹³⁸A. Beveratos, R. Brouri, T. Gacoin, A. Villing, J.-P. Poizat, and P. Grangier, *Phys. Rev. Lett.* **89**, 187901 (2002).
- ¹³⁹X. Brokmann, E. Giacobino, M. Dahan, and J. Hermier, *Appl. Phys. Lett.* **85**, 712 (2004).
- ¹⁴⁰A. J. Bennett, D. C. Unitt, P. Atkinson, D. A. Ritchie, and A. J. Shields, *Opt. Express* **13**, 50 (2005).
- ¹⁴¹M. Keller, B. Lange, K. Hayasaka, W. Lange, and H. Walther, *Nature (London)* **431**, 1075 (2004).
- ¹⁴²J. McKeever, A. Boca, A. D. Boozer, R. Miller, J. R. Buck, A. Kuzmich, and H. J. Kimble, *Science* **303**, 1992 (2004).
- ¹⁴³M. Hijlkema, B. Weber, H. P. Specht, S. C. Webster, A. Kuhn, and G. Rempe, *Nat. Phys.* **3**, 253 (2007).
- ¹⁴⁴C. W. Chou, S. V. Polyakov, A. Kuzmich, and H. J. Kimble, *Phys. Rev. Lett.* **92**, 213601 (2004).
- ¹⁴⁵D. N. Matsukevich, T. Chaneliere, S. D. Jenkins, S.-Y. Lan, T. A.B. Kennedy, and A. Kuzmich, *Phys. Rev. Lett.* **97**, 013601 (2006).
- ¹⁴⁶P. G. Evans, R. S. Bennink, W. P. Grice, T. S. Humble, and J. Schaake, *Phys. Rev. Lett.* **105**, 253601 (2010).
- ¹⁴⁷R. J. Glauber, *Phys. Rev.* **130**, 2529 (1963).
- ¹⁴⁸R. J. Glauber, *Phys. Rev.* **131**, 2766 (1963).
- ¹⁴⁹R. Hanbury-Brown and R. Q. Twiss, *Proc. R. Soc. London, Ser. A* **242**, 300 (1957).
- ¹⁵⁰P. Michler, A. Kiraz, C. Becher, W. V. Schoenfeld, P. M. Petroff, L. Zhang, E. Hu, and A. Imamoglu, *Science* **290**, 2282 (2000).
- ¹⁵¹C. Santori, D. Fattal, J. Vučković, G. S. Solomon, and Y. Yamamoto, *Nature (London)* **419**, 594 (2002).
- ¹⁵²Z. Yuan, B. E. Kardynal, R. M. Stevenson, A. J. Shields, C. J. Lobo, K. Cooper, N. S. Beattie, D. A. Ritchie, and M. Pepper, *Science* **295**, 102 (2002).
- ¹⁵³V. Zwiller, T. Aichele, W. Seifert, J. Persson, and O. Benson, *Appl. Phys. Lett.* **82**, 1509 (2003).
- ¹⁵⁴J. Kim, O. Benson, H. Kan, and Y. Yamamoto, *Nature (London)* **397**, 500 (1999).
- ¹⁵⁵F. D. Martini, G. D. Giuseppe, and M. Marrocco, *Phys. Rev. Lett.* **76**, 900 (1996).
- ¹⁵⁶C. Brunel, B. Lounis, P. Tamarat, and M. Orrit, *Phys. Rev. Lett.* **83**, 2722 (1999).
- ¹⁵⁷B. Lounis and W. E. Moerner, *Nature (London)* **407**, 491 (2000).
- ¹⁵⁸A. Kuhn, M. Hennrich, and G. Rempe, *Phys. Rev. Lett.* **89**, 067901 (2002).
- ¹⁵⁹B. B. Blinov, D. L. Moehring, L.-M. Duan, and C. Monroe, *Nature (London)* **428**, 153 (2004).
- ¹⁶⁰C. Kurtsiefer, S. Mayer, P. Zarda, and H. Weinfurter, *Phys. Rev. Lett.* **85**, 290 (2000).
- ¹⁶¹A. Beveratos, R. Brouri, T. Gacoin, J.-P. Poizat, and P. Grangier, *Phys. Rev. A* **64**, 061802 (2001).
- ¹⁶²T. Wilk, S. C. Webster, H. P. Specht, G. Rempe, and A. Kuhn, *Phys. Rev. Lett.* **98**, 063601 (2007).
- ¹⁶³B. Dayan, A. S. Parkins, T. Aoki, E. P. Ostby, K. J. Vahala, and H. J. Kimble, *Science* **319**, 1062 (2008).
- ¹⁶⁴T. Aoki, A. S. Parkins, D. J. Alton, C. A. Regal, B. Dayan, E. Ostby, K. J. Vahala, and H. J. Kimble, *Phys. Rev. Lett.* **102**, 083601 (2009).
- ¹⁶⁵U. Gaubatz, P. Rudecki, M. Becker, S. Schiemann, M. Kütz, and K. Bergmann, *Chem. Phys. Lett.* **149**, 463 (1988).
- ¹⁶⁶L. M. Duan, A. Kuzmich, and H. J. Kimble, *Phys. Rev. A* **67**, 032305 (2003).
- ¹⁶⁷H. G. Barros, A. Stute, T. E. Northup, C. Russo, P. O. Schmidt, and R. Blatt, *New J. Phys.* **11**, 103004 (2009).
- ¹⁶⁸D. Kielpinski, C. Monroe, and D. Wineland, *Nature (London)* **417**, 709 (2002).
- ¹⁶⁹M. Riebe, T. Monz, K. Kim, A. S. Villar, P. Schindler, M. Chwalla, M. Hennrich, and R. Blatt, *Nat. Phys.* **4**, 839 (2008).
- ¹⁷⁰J. P. Home, D. Hanneke, J. D. Jost, J. M. Amini, D. Leibfried, and D. J. Wineland, *Science* **325**, 1227 (2009).
- ¹⁷¹S. Kitson, P. Jonsson, J. Rarity, and P. Tapster, *Phys. Rev. A* **58**, 620 (1998).
- ¹⁷²A. Kiraz, S. Falth, C. Becher, B. Gayra, W. V. Schoenfeld, P. M. Petroff, L. Zhang, E. Hu, and A. Imamoglu, *Phys. Rev. B* **65**, 161303R (2002).
- ¹⁷³A. Kiraz, M. Ehrl, T. Hellerer, O. E. Mustecaplioglu, C. Brauchle, and A. Zumbusch, *Phys. Rev. Lett.* **94**, 223602 (2005).
- ¹⁷⁴L. Fleury, J. Segura, G. Zumofen, B. Hecht, and U. Wild, *Phys. Rev. Lett.* **84**, 1148 (2000).
- ¹⁷⁵A. J. Shields, M. P. O'Sullivan, I. Farrer, D. A. Ritchie, R. A. Hogg, M. L. Leadbeater, C. E. Norman, and M. Pepper, *Appl. Phys. Lett.* **76**, 3673 (2000).
- ¹⁷⁶P. Michler, A. Imamoglu, M. Mason, P. Carson, G. Strouse, and S. Buratto, *Nature (London)* **406**, 968 (2000).
- ¹⁷⁷O. Benson, C. Santori, M. Pelton, and Y. Yamamoto, *Phys. Rev. Lett.* **84**, 2513 (2000).
- ¹⁷⁸E. Moreau, I. Robert, J. Gerard, I. Abram, L. Manin, and V. Thierry-Mieg, *Appl. Phys. Lett.* **79**, 2865 (2001).
- ¹⁷⁹C. Santori, M. Pelton, G. Solomon, Y. Dale, and E. Yamamoto, *Phys. Rev. Lett.* **86**, 1502 (2001).
- ¹⁸⁰M. Pelton, C. Santori, J. Vuckovic, B. Zhang, G. Solomon, J. Plant, and Y. Yamamoto, *Phys. Rev. Lett.* **89**, 233602 (2002).
- ¹⁸¹C. Unitt, A. Bennett, P. Atkinson, K. Cooper, P. See, D. Gevaux, M. Ward, R. Stevenson, D. Ritchie, and A. Shields, *J. Opt. B: Quantum Semiclassical Opt.* **7**, S129 (2005).
- ¹⁸²A. Kress, F. Hofbauer, N. Reinelt, M. Kaniber, H. Krenner, R. Meyer, G. Bohm, and J. Finley, *Phys. Rev. B* **71**, 241304(R) (2005).
- ¹⁸³S. Laurent, S. Varoutsis, L. Le Gratiet, A. Lemaitre, I. Sagnes, F. Raineri, A. Levenson, I. Robert-Philip, and I. Abram, *Appl. Phys. Lett.* **87**, 163107 (2005).
- ¹⁸⁴D. Press, S. Goetzinger, S. Reitzenstein, C. Hofmann, A. Loeffler, M. Kamp, A. Forchel, and Y. Yamamoto, *Phys. Rev. Lett.* **98**, 117402 (2007).
- ¹⁸⁵M. B. Ward, T. Farrow, P. See, Z. L. Yuan, O. Z. Karimov, A. J. Bennett, A. J. Shields, P. Atkinson, K. Cooper, and D. A. Ritchie, *Appl. Phys. Lett.* **90**, 063512 (2007).
- ¹⁸⁶D. Leonard, M. Krishnamurthy, C. M. Reaves, S. P. Denbaars, and P. M. Petroff, *Appl. Phys. Lett.* **63**, 3203 (1993).
- ¹⁸⁷C. M. Santori, Ph.D. dissertation, Stanford University, 2003.
- ¹⁸⁸E. M. Purcell, *Phys. Rev.* **69**, 681 (1946).
- ¹⁸⁹A. Muller, W. Fang, J. Lawall, and G. S. Solomon, *Phys. Rev. Lett.* **103**, 217402 (2009).
- ¹⁹⁰E. B. Flagg, A. Muller, S. V. Polyakov, A. Ling, A. Migdall, and G. S. Solomon, *Phys. Rev. Lett.* **104**, 137401 (2010).
- ¹⁹¹R. B. Patel, A. J. Bennett, I. Farrer, C. A. Nicoll, D. A. Ritchie, and A. J. Shields, *Nature Photon.* **4**, 632 (2010).
- ¹⁹²R. Brouri, A. Beveratos, J.-P. Poizat, and P. Grangier, *Opt. Lett.* **25**, 1294 (2000).
- ¹⁹³S. Pezzagna, D. Rogalla, D. Wildanger, J. Meijer, and A. Zaitsev, *New J. Phys.* **13**, 035024 (2011).
- ¹⁹⁴P. Tamarat, T. Gaebel, J. R. Rabeau, M. Khan, A. D. Greentree, H. Wilson, L. C.L. Hollenberg, S. Praver, P. Hemmer, F. Jelezko, J. Wrachtrup, *Phys. Rev. Lett.* **97**, 083002 (2006).
- ¹⁹⁵P. E. Barclay, K.-M. C. Fu, C. Santori, and R. G. Beausoleil, *Appl. Phys. Lett.* **95**, 191115 (2009).
- ¹⁹⁶C. H. van der Wal, M. D. Eisaman, A. Andre, R. L. Walsworth, D. F. Phillips, A. S. Zibrov, and M. D. Lukin, *Science* **301**, 196 (2003).
- ¹⁹⁷A. Kuzmich, W. P. Bowen, A. D. Boozer, A. Boca, C. W. Chou, L.-M. Duan, and H. J. Kimble, *Nature (London)* **423**, 731 (2003).
- ¹⁹⁸R. Zhao, Y. O. Dudin, S. D. Jenkins, C. J. Campbell, D. N. Matsukevich, T. A.B. Kennedy, and A. Kuzmich, *Nat. Phys.* **5**, 100 (2009).
- ¹⁹⁹B. Zhao, Y.-A. Chen, X.-H. Bao, T. Strassel, C.-S. Chuu, X.-M. Jin, J. Schmiedmayer, Z.-S. Yuan, S. Chen, and J.-W. Pan, *Nat. Phys.* **5**, 95 (2009).
- ²⁰⁰E. S. Fry, *Phys. Rev. A* **8**, 1219 (1973).
- ²⁰¹W. Louisell, A. Siegman, and A. Yariv, *Phys. Rev.* **124**, 1646 (1961).
- ²⁰²B. Y. Zeldovich and D. N. Klyshko, *JETP Lett.* **9**, 40 (1969) [http://www.jetpletters.ac.ru/ps/1639/article_25275.pdf].
- ²⁰³D. Burnham and D. Weinberg, *Phys. Rev. Lett.* **25**, 84 (1970).
- ²⁰⁴L. Mandel and E. Wolf, *Optical Coherence and Quantum Optics* (Cambridge University Press, New York, 1995).
- ²⁰⁵R. W. Boyd, *Nonlinear Optics*, 2nd ed. (Academic, San Diego, 2003).
- ²⁰⁶J. Chen, A. J. Pearlman, A. Ling, J. Fan, and A. Migdall, *Opt. Express* **17**, 6727 (2009).
- ²⁰⁷J. A. Armstrong, N. Bloembergen, J. Ducuing, and P. S. Pershan, *Phys. Rev.* **127**, 1918 (1962).
- ²⁰⁸A. Peres, *Phys. Rev. Lett.* **77**, 1413 (1996).
- ²⁰⁹C. K. Law, I. A. Walmsley, and J. H. Eberly, *Phys. Rev. Lett.* **84**, 5304 (2000).

- ²¹⁰W. P. Grice, A. B. U'Ren, and I. A. Walmsley, *Phys. Rev. A* **64**, 063815 (2001).
- ²¹¹P. J. Mosley, J. S. Lundeen, B. J. Smith, and I. A. Walmsley, *New J. Phys.* **10**, 093011 (2008).
- ²¹²S. Tanzilli, H. de Riedmatten, W. Tittel, H. Zbinden, P. Baldi, M. de Micheli, D. B. Ostrowski, and N. Gisin, *Electron. Lett.* **37**, 26 (2001).
- ²¹³S. Tanzilli, W. Tittel, H. de Riedmatten, H. Zbinden, P. Baldi, M. de Micheli, D. B. Ostrowski, and N. Gisin, *Eur. Phys. J. D* **18**, 155 (2002).
- ²¹⁴E. J. Mason, M. A. Albota, F. König, and F. N.C. Wong, *Opt. Lett.* **27**, 2115 (2002).
- ²¹⁵O. Alibart, D. B. Ostrowski, P. Baldi, and S. Tanzilli, *Opt. Lett.* **30**, 1539 (2005).
- ²¹⁶Y.-P. Huang, J. B. Altepeter, and P. Kumar, *Phys. Rev. A* **82**, 043826 (2010).
- ²¹⁷M. Fiorentino, S. M. Spillane, R. G. Beausoleil, T. D. Roberts, P. Battle, and M. W. Munro, *Opt. Express* **15**, 7479 (2007).
- ²¹⁸T. Zhong, F. N. Wong, T. D. Roberts, and P. Battle, *Opt. Express* **17**, 12019 (2009).
- ²¹⁹Z. H. Levine, J. Fan, J. Chen, A. Ling, and A. Migdall, *Opt. Express* **18**, 3708 (2010).
- ²²⁰J. E. Sharping, M. Fiorentino, and P. Kumar, *Opt. Lett.* **26**, 367 (2001).
- ²²¹M. Fiorentino, P. L. Voss, J. E. Sharping, and P. Kumar, *IEEE Photonics Technol. Lett.* **14**, 983 (2002).
- ²²²X. Li, P. L. Voss, J. E. Sharping, and P. Kumar, *Phys. Rev. Lett.* **94**, 053601 (2005).
- ²²³J. Rarity, J. Fulconis, J. Dulgall, W. Wadsworth, and P. Russell, *Opt. Express* **13**, 534 (2005).
- ²²⁴J. Fan, A. Dogariu, and L. J. Wang, *Opt. Lett.* **30**, 1530 (2005).
- ²²⁵J. Fan, A. Migdall, and L. J. Wang, *Opt. Lett.* **30**, 3368 (2005).
- ²²⁶J. Fan and A. Migdall, *Opt. Lett.* **31**, 2771 (2006).
- ²²⁷T. Tsuchizawa, K. Yamada, H. Fukuda, T. Watanabe, J. Takahashi, M. Takahashi, T. Shoji, E. Tamechika, S. Itabashi, and H. Morita, *IEEE J. Sel. Top. Quantum Electron.* **11**, 232 (2005).
- ²²⁸J. E. Sharping, K. F. Lee, M. A. Foster, A. C. Turner, B. S. Schmidt, M. Lipson, A. L. Gaeta, and P. Kumar, *Opt. Express* **14**, 12388 (2006).
- ²²⁹K.-i. Harada, H. Takesue, H. Fukuda, T. Tsuchizawa, T. Watanabe, K. Yamada, Y. Tokura, and S.-i. Itabashi, *Opt. Express* **16**, 20368 (2008).
- ²³⁰H. Takesue and K. Inoue, *Opt. Express* **13**, 7832 (2005).
- ²³¹K. F. Lee, J. Chen, C. Liang, X. Li, P. L. Voss, and P. Kumar, *Opt. Lett.* **31**, 1905 (2006).
- ²³²O. Kuzucu and F. N.C. Wong, *Phys. Rev. A* **77**, 032314 (2008).
- ²³³A. L. Migdall, D. Branning, and S. Castelletto, *Phys. Rev. A* **66**, 053805 (2002).
- ²³⁴M. J. Fitch, B. C. Jacobs, T. B. Pittman, and J. D. Franson, *Phys. Rev. A* **68**, 043814 (2003).
- ²³⁵E. Jeffrey, N. A. Peters, and P. G. Kwiat, *New J. Phys.* **6**, 100 (2004).
- ²³⁶J. H. Shapiro and F. Wong, *Opt. Lett.* **32**, 2698 (2007).
- ²³⁷T. Pittman, B. Jacobs, and J. Franson, *Phys. Rev. A* **66**, 042303 (2002).
- ²³⁸T. Pittman and J. Franson, *Phys. Rev. A* **66**, 062302 (2002).
- ²³⁹P. M. Leung and T. C. Ralph, *Phys. Rev. A* **74**, 022311 (2006).
- ²⁴⁰K. T. McCusker, N. A. Peters, A. P. VanDevender, and P. G. Kwiat, "A Deterministic Single-Photon Source," in *Conference on Lasers and Electro-optics/Quantum Electronics and Laser Science Conference and Photonic Applications Systems Technologies*, OSA Technical Digest (CD) (Optical Society of America, 2008), paper JTuA117.
- ²⁴¹A. I. Lvovsky, B. C. Sanders, and W. Tittel, *Nature Photon.* **3**, 706 (2009).
- ²⁴²O. Cohen, J. S. Lundeen, B. J. Smith, G. Puentes, P. J. Mosley, and I. A. Walmsley, *Phys. Rev. Lett.* **102**, 123603 (2009).
- ²⁴³T. B. Pittman and J. D. Franson, *Phys. Rev. A* **74**, 041801(R) (2006).
- ²⁴⁴I. Afek, O. Ambar, and Y. Silberberg, *Science* **328**, 879 (2010).
- ²⁴⁵H.-A. Bachor and T. C. Ralph, *A Guide to Experiments in Quantum Optics* (Wiley VCH, Berlin, 2004), Chap. 7.
- ²⁴⁶S. Cova, M. Ghioni, A. Lotito, I. Rech, and F. Zappa, *J. Mod. Opt.* **51**, 1267 (2004).
- ²⁴⁷A. Lacaita, F. Zappa, S. Cova, and P. Lovati, *Appl. Opt.* **35**, 2986 (1996).
- ²⁴⁸G. Ribordy, N. Gisin, O. Guinnard, D. Stucki, M. Wegmuller, and H. Zbinden, *J. Mod. Opt.* **51**, 1381 (2004).
- ²⁴⁹Z. L. Yuan, B. E. Kardynal, A. W. Sharpe, and A. J. Shields, *Appl. Phys. Lett.* **91**, 041114 (2007).
- ²⁵⁰A. Lacaita, P. A. Francese, F. Zappa, and S. Cova, *Appl. Opt.* **33**, 6902 (1994).
- ²⁵¹D. M. Taylor, J. C. Jackson, A. P. Morrison, A. Mathewson, and J. G. Rarity, *J. Mod. Opt.* **51**, 1323 (2004).
- ²⁵²S. Komiyama, O. Astafiev, V. Antonov, T. Kutsuwa, and H. Hirai, *Nature (London)* **403**, 405 (2000).
- ²⁵³K. M. Rosfjord, J. K.W. Yang, E. A. Dauler, A. J. Kerman, V. Anant, B. M. Voronov, G. N. Gol'tsman, and K. K. Berggren, *Opt. Express* **14**, 527 (2006).
- ²⁵⁴M. A. Albota and F. N.C. Wong, *Opt. Lett.* **29**, 1449 (2004).
- ²⁵⁵H. Takesue, E. Diamanti, C. Langrock, M. M. Fejer, and Y. Yamamoto, *Opt. Express* **14**, 13067 (2006).
- ²⁵⁶R. Thew, S. Tanzilli, L. Krainer, S. Zeller, A. Rochas, I. Rech, S. Cova, H. Zbinden, and N. Gisin, *New J. Phys.* **8**, 32 (2006).
- ²⁵⁷D. Rosenberg, A. E. Lita, A. J. Miller, and S. W. Nam, *Phys. Rev. A* **71**, 061803(R) (2005).
- ²⁵⁸A. Peacock, P. Verhoeve, N. Rando, A. van Dordrecht, B. G. Taylor, C. Erd, M. A.C. Perryman, R. Venn, J. Howlett, D. J. Goldie, J. Lumley, and M. Wallis, *Nature (London)* **381**, 135 (1996).
- ²⁵⁹A. Peacock, P. Verhoeve, N. Rando, A. van Dordrecht, B. G. Taylor, C. Erd, M. A.C. Perryman, R. Venn, J. Howlett, D. J. Goldie, J. Lumley, and M. Wallis, *J. Appl. Phys.* **81**, 7641 (1997).
- ²⁶⁰P. Verhoeve, N. Nando, A. Peacock, A. van Dordrecht, A. Poelaert, D. Goldie, and R. Venn, *J. Appl. Phys.* **83**, 6118 (1998).
- ²⁶¹S. Friedrich, *J. Low Temp. Phys.* **151**, 277 (2008).
- ²⁶²A. Divochiy, F. Marsili, D. Bitauld, A. Gaggero, R. Leoni, F. Mattioli, A. Korneev, V. Seleznev, N. Kurova, O. Minaeva, G. Gol'tsman, K. G. Lagoudakis, M. Benkhaoul, F. Lévy, and A. Fiore, *Nature Photon.* **2**, 302 (2008).
- ²⁶³M. Fujiwara and M. Sasaki, *Appl. Opt.* **46**, 3069 (2007).
- ²⁶⁴E. Waks, K. Inoue, W. D. Oliver, E. Diamanti, and Y. Yamamoto, *IEEE J. Sel. Top. Quantum Electron.* **9**, 1502 (2003).
- ²⁶⁵E. J. Gansen, M. A. Rowe, M. B. Greene, D. Rosenberg, T. E. Harvey, M. Y. Su, R. H. Hadfield, S. W. Nam, and R. P. Mirin, *Nature Photon.* **1**, 585 (2007).
- ²⁶⁶D. Achilles, C. Silberhorn, C. Sliwa, K. Banaszek, I. A. Walmsley, M. J. Fitch, B. C. Jacobs, T. B. Pittman, and J. D. Franson, *J. Mod. Opt.* **51**, 1499 (2004).
- ²⁶⁷B. E. Kardynal, Z. L. Yuan, and A. J. Shields, *Nature Photon.* **2**, 425 (2008).
- ²⁶⁸A. Gulian, K. Wood, D. van Vechten, and G. Fritz, *J. Mod. Opt.* **15**, 1467 (2004).
- ²⁶⁹D. James and P. Kwiat, *Phys. Rev. Lett.* **89**, 183601 (2002).
- ²⁷⁰W. J. Munro, K. Nemoto, R. G. Beausoleil, and T. P. Spiller, *Phys. Rev. A* **71**, 033819 (2005).
- ²⁷¹See <http://jp.hamamatsu.com/resources/products/etd/pdf/m-h7422e.pdf> (2010) for an example of a visible PMT commercially packaged as a photon-counting module including voltage bias electronics and thermoelectric cooling.
- ²⁷²Certain commercial equipment, instruments or materials are identified in this paper to foster understanding. Such identification does not imply recommendation or endorsement by the National Institute of Standards and Technology, nor does it imply that the materials or equipment are necessarily the best available for the purpose.
- ²⁷³See http://jp.hamamatsu.com/resources/products/etd/pdf/NIR-PMT-APPLI_TPMO1040E02.pdf (2010) for an example of a near IR PMT commercially packaged as a photon-counting module including voltage bias electronics and thermoelectric cooling.
- ²⁷⁴See http://excelitas.com/ProductPages/Single_Photon_Counting_Modules_SPCM.aspx (2011) for an example of a visible thick junction SPAD commercially packaged as a photon-counting module including voltage bias electronics and thermoelectric cooling.
- ²⁷⁵See http://www.microphotondevices.com/media/pdf/PDM_v3_6.pdf (2011) for an example of a visible thin-junction SPAD commercially packaged as a photon-counting module including voltage bias electronics and thermoelectric cooling.
- ²⁷⁶O. Thomas, Z. L. Yuan, J. F. Dynes, A. W. Sharpe, and A. J. Shields, *Appl. Rev. Lett.* **97**, 031102 (2010).
- ²⁷⁷M. Akiba, K. Tsujino, and M. Sasaki, *Opt. Lett.* **35**, 2621 (2010).
- ²⁷⁸M. Ghioni, G. Armellini, P. Maccagnani, I. Rech, M. K. Emsley, and M. S. Unlu, *J. Mod. Opt.* **56**, 309 (2009).
- ²⁷⁹D. A. Kalashnikov, S. H. Tan, M. V. Chekhova, and L. A. Krivitsky, *Opt. Express* **19**, 9352 (2011).
- ²⁸⁰See http://jp.hamamatsu.com/resources/products/ssd/pdf/s10362-11-series_kapd1022e05.pdf (2009) for an example of a commercial visible multipixel SPAD.
- ²⁸¹R. A. LaRue, G. A. Davis, D. Pudvay, K. A. Costello, and V. W. Aebi, *IEEE Elect. Dev. Lett.* **20**, 126 (1999).

- ²⁸²N. Bertone, R. Biasi, and B. Dion, *Proc. SPIE* **5726**, 153 (2005).
- ²⁸³M. Micuda, O. Haderka, and M. Jezek, *Phys. Rev. A* **78**, 025804 (2008).
- ²⁸⁴L. A. Jiang, E. A. Dauler, and J. T. Chang, *Phys. Rev. A* **75**, 062325 (2007).
- ²⁸⁵G. Brida, I. P. Degiovanni, F. Piacentini, V. Schettini, S. V. Polyakov, and A. Migdall, *Rev. Sci. Instrum.* **80**, 116103 (2009).
- ²⁸⁶C. Gobby, Z. L. Yuan, and A. J. Shields, *Appl. Phys. Lett.* **84**, 3762 (2004).
- ²⁸⁷A. R. Dixon, Z. L. Yuan, J. F. Dynes, A. W. Sharpe, and A. J. Shields, *Opt. Express* **16**, 18790 (2008).
- ²⁸⁸A. Yoshizawa, R. Kaji, and H. Tsuchida, *Appl. Phys. Lett.* **84**, 3606 (2004).
- ²⁸⁹X. Jiang, M. A. Itzler, B. Nyman, and K. Slomkowski, *Proc. SPIE* **7320**, 732011 (2009).
- ²⁹⁰P. Lightwave (2010), see http://www.princetonlightwave.com/content/PNA-20XNFADDatashet_rv2.pdf.
- ²⁹¹K. Zhao, A. Zhang, Y. hwa Lo, and W. Farr, *Appl. Phys. Lett.* **91**, 081107 (2007).
- ²⁹²H. Takesue, E. Diamanti, T. Honjo, C. Langrock, M. M. Fejer, K. Inoue, and Y. Yamamoto, *New J. Phys.* **7**, 232 (2005).
- ²⁹³A. P. Van Devender and P. G. Kwiat, *J. Opt. Soc. Am. B* **24**, 295 (2007).
- ²⁹⁴H. Xu, L. Ma, A. Mink, B. Hershman, and X. Tang, *Opt. Express* **15**, 7247 (2007).
- ²⁹⁵S. Takeuchi, J. Kim, Y. Yamamoto, and H. H. Hogue, *Appl. Phys. Lett.* **74**, 1063 (1999).
- ²⁹⁶B. Baek, K. McKay, M. Stevens, J. K.H. Hogue, and S. W. Nam, *IEEE J. Quantum Electron.* **46**, 991 (2010).
- ²⁹⁷P. G. Kwiat, A. M. Steinberg, R. Y. Chiao, P. H. Eberhard, and M. D. Petroff, *Appl. Opt.* **33**, 1844 (1994).
- ²⁹⁸D. Rosenberg, J. W. Harrington, P. R. Rice, P. A. Hiskett, C. G. Peterson, R. J. Hughes, A. E. Lita, S. W. Nam, and J. E. Nordholt, *Phys. Rev. Lett.* **98**, 010503 (2007).
- ²⁹⁹A. E. Lita, A. J. Miller, and S. W. Nam, *Opt. Express* **16**, 3032 (2008).
- ³⁰⁰A. E. Lita, B. Calkins, L. A. Pellochoud, A. J. Miller, and S. Nam, *AIP Conf. Proc.* **1185**, 351 (2009).
- ³⁰¹D. Fukuda, G. Fujii, T. Numata, A. Yoshizawa, H. Tsuchida, H. Fujino, H. Ishii, T. Itatani, S. Inoue, and T. Zama, *Metrologia* **46**, S288 (2009).
- ³⁰²D. Fukuda, G. Fujii, T. Numata, A. Yoshizawa, H. Tsuchida, H. Fujino, H. Ishii, T. Itatani, S. Inoue, and T. Zama, Tenth International Conference on Quantum Communication, Measurement and Computation (QCMC), Brisbane, Queensland, Australia, 2010.
- ³⁰³D. Fukuda, G. Fujii, T. Numata, K. Amemiya, A. Yoshizawa, H. Tsuchida, H. Fujino, H. Ishii, T. Itatani, S. Inoue, and T. Zama, *Opt. Express* **19**, 870 (2011).
- ³⁰⁴H. Takesue, S. W. Nam, Q. Zhang, R. H. Hadfield, T. Honjo, K. Tamaki, and Y. Yamamoto, *Nature Photon.* **1**, 343 (2007).
- ³⁰⁵T. Peacock, P. Verhoeve, N. Rando, C. Erd, M. Bavdaz, B. Taylor, and D. Perez, *Astron. Astrophys., Suppl. Ser.* **127**, 497 (1998).
- ³⁰⁶J. C. Blakesley, P. See, A. J. Shields, B. E. Kardyna, P. Atkinson, I. Farrer, and D. A. Ritchie, *Phys. Rev. Lett.* **94**, 067401 (2005).
- ³⁰⁷M. A. Rowe, E. J. Gansen, M. Greene, R. H. Hadfield, T. E. Harvey, M. Y. Su, S. W. Nam, R. P. Mirin, and D. Rosenberg, *Appl. Phys. Lett.* **89**, 253505 (2006).
- ³⁰⁸M. A. Rowe, G. M. Salley, E. J. Gansen, S. M. Etzel, S. W. Nam, and R. P. Mirin, *J. Appl. Phys.* **107**, 063110 (2010).
- ³⁰⁹R. Hadfield, *Nature Photon.* **3**, 696 (2009).
- ³¹⁰R. E. Simon, A. H. Sommer, J. A. Tietjen, and B. F. Williams, *Appl. Phys. Lett.* **13**, 355 (1968).
- ³¹¹G. A. Morton, H. M. Smith, and H. R. Krall, *Appl. Phys. Lett.* **13**, 356 (1968).
- ³¹²A. Nevet, A. Hayat, and M. Orenstein, *Opt. Lett.* **36**, 725 (2011).
- ³¹³M. A. Itzler, R. Ben-Michael, C. F. Hsu, K. Slomkowski, A. Tosi, S. Cova, F. Zappa, and R. Ispasoiu, *J. Mod. Opt.* **54**, 283 (2007).
- ³¹⁴H. Kosaka, D. S. Rao, H. D. Robinson, P. Bandaru, T. Sakamoto, and E. Yablonovitch, *Phys. Rev. B* **65**, 201307 (2002).
- ³¹⁵G. Gol'tsman, O. Okunev, G. Chulkova, A. Lipatov, A. Dzardanov, K. Smirnov, A. Semenov, B. Voronov, C. Williams, and R. Sobolewski, *IEEE Trans. Appl. Supercond.* **11**, 574 (2001).
- ³¹⁶G. Gol'tsman, O. Okunev, G. Chulkova, A. Lipatov, A. Semenov, K. Smirnov, B. Voronov, A. Dzardanov, C. Williams, and R. Sobolewski, *Appl. Phys. Lett.* **79**, 705 (2001).
- ³¹⁷S. Miki, M. Fujiwara, M. Sasaki, B. Baek, A. J. Miller, R. H. Hadfield, S. W. Nam, and Z. Wang, *Appl. Phys. Lett.* **92**, 061116 (2008).
- ³¹⁸V. Anant, A. J. Kerman, E. A. Dauler, J. K. Yang, K. M. Rosfjord, and K. K. Berggren, *Opt. Express* **16**, 10750 (2008).
- ³¹⁹E. A. Dauler, A. J. Kerman, B. S. Robinson, J. K.W. Yang, G. G. B. Voronov, S. A. Hamilton, and K. K. Berggren, *J. Mod. Opt.* **56**, 364 (2009).
- ³²⁰J. K.W. Yang, A. J. Kerman, E. A. Dauler, V. Anant, K. M. Rosfjord, and K. K. Berggren, *IEEE Trans. Appl. Supercond.* **17**, 581 (2007).
- ³²¹A. P. VanDevender and P. G. Kwiat, *J. Mod. Opt.* **51**, 1433 (2004).
- ³²²D. Herr, see <http://lepton-tech.com/pdf/counterdatashet12-10-08.pdf> (2008) for an example of a commercial IR up-conversion photon-counting module using a PMT to detect the up-converted photon.
- ³²³H. Xu, L. Ma, A. Mink, B. Hershman, and X. Tang, *Phys. Rev. A* **72**, 052311 (2005).
- ³²⁴E. Knill, R. Laflamme, and G. J. Milburn, *Nature (London)* **409**, 46 (2001).
- ³²⁵A. J. Kerman, E. A. Dauler, W. E. Keicher, J. K.W. Yang, K. K. Berggren, G. Goltsman, and B. Voronov, *Appl. Phys. Lett.* **88**, 111116 (2006).
- ³²⁶B. Cabrera, R. M. Clarke, P. Colling, A. J. Miller, S. Nam, and R. W. Romani, *Appl. Phys. Lett.* **73**, 735 (1998).
- ³²⁷D. Fukuda, G. Fujii, A. Yoshizawa, H. Tsuchida, R. M.T. Damayanthi, H. Takahashi, S. Inoue, and M. Ohkubo, *J. Low Temp. Phys.* **151**, 100 (2008).
- ³²⁸A. J. Miller, A. E. Lita, B. Calkins, I. Vayshenker, S. M. Gruber, and S. W. Nam, *Opt. Express* **19**, 9102 (2011).
- ³²⁹K. Banaszek and I. A. Walmsley, *Opt. Lett.* **28**, 52 (2003).
- ³³⁰A. Imamoglu, *Phys. Rev. Lett.* **89**, 163602 (2002).
- ³³¹N. Imoto, H. A. Haus, and Y. Yamamoto, *Phys. Rev. A* **32**, 2287 (1985).
- ³³²P. Kok, H. Lee, and J. P. Dowling, *Phys. Rev. A* **66**, 063814 (2002).
- ³³³A. D. Greentree, R. G. Beausoleil, L. C.L. Hollenberg, W. J. Munro, K. Nemoto, S. Praver, and T. P. Spiller, *New J. Phys.* **11**, 093005 (2009).
- ³³⁴Q. A. Turchette, C. J. Hood, W. Lange, H. Mabuchi, and H. J. Kimble, *Phys. Rev. Lett.* **75**, 4710 (1995).
- ³³⁵T. J. Kippenberg, S. M. Spillane, and K. J. Vahala, *Phys. Rev. Lett.* **93**, 083904 (2004).
- ³³⁶G. J. Pryde, J. L. O'Brien, A. G. White, S. D. Bartlett, and T. C. Ralph, *Phys. Rev. Lett.* **92**, 190402 (2004).
- ³³⁷P. Kok and W. J. Munro, *Phys. Rev. Lett.* **95**, 048901 (2005).
- ³³⁸G. J. Pryde, J. L. O'Brien, A. G. White, S. D. Bartlett, and T. C. Ralph, *Phys. Rev. Lett.* **95**, 048902 (2005).
- ³³⁹R. H. Haitz, *J. Appl. Phys.* **35**, 1370 (1964).
- ³⁴⁰R. H. Haitz, *J. Appl. Phys.* **36**, 3123 (1965).
- ³⁴¹A. Lacaita, S. Longhi, and A. Spinelli, in *Proceedings of the International Conference on Applications of Photonic Technology*, edited by G. A. Lampropoulos, J. Chrostowski, and R. M. Measures (Plenum, London, 1994).
- ³⁴²A. Lacaita, A. Spinelli, and S. Longhi, *Appl. Phys. Lett.* **67**, 2627 (1995).
- ³⁴³W. Nicholson, *Nuclear Electronics* (Wiley, New York, 1974).
- ³⁴⁴M. A. Itzler, X. Jiang, B. Nyman, and K. Slomkowski, *Proc. SPIE* **7222**, 72221K (2000).
- ³⁴⁵P. Antognetti, S. Cova, and A. Longoni, in *Proceedings of the Second Ispra Nuclear Electronics Symposium* (Office for Official Publications of the European Communities, Luxembourg, Belgium, 1975), EURATOM Publ. EUR 537e.
- ³⁴⁶S. Cova, A. Longoni, and A. Andreoni, *Rev. Sci. Instrum.* **52**, 408 (1981).
- ³⁴⁷S. Cova, A. Longoni, and G. Ripamonti, *IEEE Trans. Nucl. Sci.* **29**, 599 (1982).
- ³⁴⁸M. Ware, A. Migdall, J. C. Bienfang, and S. V. Polyakov, *J. Mod. Opt.* **54**, 361 (2007).
- ³⁴⁹S. Cova, M. Ghioni, A. Lacaita, C. Samori, and F. Zappa, *Appl. Opt.* **35**, 1956 (1996).
- ³⁵⁰A. Tosi, A. Gallivanoni, F. Zappa, and S. Cova, *Proc. SPIE* **6372**, 63720Q (2006).
- ³⁵¹F. Zappa, A. Giudice, M. Ghioni, and S. Cova, in *Proc. of the 28th European Solid-State Circuits Conference, ESSCIRC* (2002), Florence, Italy, p. 355, see http://ieeexplore.ieee.org/xpls/abs_all.jsp?arnumber=1471538.
- ³⁵²D. S. Bethune and W. P. Risk, *IEEE J. Quantum Electron.* **36**, 340 (2000).
- ³⁵³A. Tomita and K. Nakamura, *Opt. Lett.* **27**, 1827 (2002).
- ³⁵⁴Z. J. Wei, P. Zhou, and J. D. Wang, *J. Phys. D: Appl. Phys.* **40**, 6922 (2007).
- ³⁵⁵A. Yoshizawa, R. Kaji, and H. Tsuchida, *Jpn. J. Appl. Phys.* **43**, L735 (2004).
- ³⁵⁶H. Finkelstein, M. Gross, Y.-H. Lo, and S. Esener, *IEEE J. Sel. Top. Quantum Electron.* **13**, 959 (2007).
- ³⁵⁷M. Ghioni, S. Cova, F. Zappa, and C. Samori, *Rev. Sci. Instrum.* **67**, 3440 (1996).

- ³⁵⁸H.-K. Lo, X. Ma, and K. Chen, *Phys. Rev. Lett.* **94**, 230504 (2005).
- ³⁵⁹T. Schmitt-Manderbach, H. Weier, M. Furst, R. Ursin, F. Tiefenbacher, T. Scheidl, J. Perdigues, Z. Sodnik, C. Kurtsiefer, J. G. Rarity, A. Zeilinger, and H. Weinfurter, *Phys. Rev. Lett.* **98**, 010504 (2007).
- ³⁶⁰V. Makarov, A. Anisimov, and J. Skaar, *Phys. Rev. A* **74**, 022313 (2006).
- ³⁶¹A. Lamas-Linares and C. Kurtsiefer, *Opt. Express* **15**, 9388 (2007).
- ³⁶²V. Makarov, *New J. Phys.* **11**, 065003 (2009).
- ³⁶³V. Burenkov, B. Qi, B. Fortescue, and H.-K. Lo (2010), see <http://arxiv.org/abs/1005.0272>.
- ³⁶⁴N. Sangouard, C. Simon, J. Min, H. Zbinden, H. de Riedmatten, and N. Gisin, *Phys. Rev. A* **76**, 050301(R) (2007).
- ³⁶⁵I. Marcikic, H. de Riedmatten, W. Tittel, H. Zbinden, M. Legre, and N. Gisin, *Phys. Rev. Lett.* **93**, 180502 (2004).
- ³⁶⁶E. Waks, K. Inoue, C. Santori, D. Fattal, J. Vuckovic, G. S. Solomon, and Y. Yamamoto, *Nature (London)* **420**, 762 (2002).
- ³⁶⁷A. R. Beaumont, J. Y. Cheung, C. J. Chunnillall, J. Ireland, and M. G. White, *Nucl. Instrum. Methods Phys. Res. A* **610**, 183 (2009).
- ³⁶⁸J. G. Rarity, P. R. Tapster, and E. Jakeman, *Opt. Commun.* **62**, 201 (1987).